**Collagen Implants to Promote Regeneration of the Adult Rat Spinal Cord**

by

Rahmatullah H. Cholas

B.S. Aerospace Engineering
Embry-Riddle Aeronautical University, 2002

SUBMITTED TO THE DEPARTMENT OF MECHANICAL ENGINEERING IN PARTIAL FULFILLMENT OF THE REQUIREMENTS OF THE DEGREE OF

MASTER OF SCIENCE IN MECHANICAL ENGINEERING
AT THE
MASSACHUSETTS INSTITUE OF TECHNOLOGY

JUNE 2006



Signature of Author:_____
Department of Mechanical Engineering
May 12, 2006

Certified by:_____
Myron Spector, Ph.D.
Senior Lecturer, Department of Mechanical Engineering, MIT
Professor of Orthopedic Surgery (Biomaterials), Harvard Medical School
Thesis Supervisor

Accepted by:_____
Lallit Anand, Ph.D.
Professor of Mechanical Engineering
Chairman, Mechanical Engineering Graduate Committee

**Collagen Implants to Promote Regeneration of the Adult Rat Spinal Cord**

by

Rahmatullah H. Cholas

Submitted to the Department of Mechanical Engineering
on May 12, 2006 in Partial Fulfillment of the
Requirements for the Degree of Master of Science in
Mechanical Engineering

## ABSTRACT

Over 250,000 people in the United States currently live with a spinal cord injury and approximately 11,000 new cases occur every year. People with spinal cord injuries experience a significant reduction in quality of life due to the many problems that arise from damage to the spinal cord including paralysis and loss of sensation below the location of injury, loss of bowel and bladder function, loss of sexual function, and impaired respiration. Despite considerable ongoing research in the area of nerve regeneration by various institutions, satisfactory treatment for spinal cord injury has not yet been discovered.

Previous studies have had considerable success in facilitating the regeneration of severed peripheral nerves through the use of collagen based implants used to bridge the resulting gap between the severed nerve stumps. The current study aims to apply this same regenerative approach to a defect created in the spinal cord of adult rats. The objective is to evaluate the efficacy of three different collagen implants toward the regeneration of the spinal cord. The experimental spinal cord injury was a complete transection at T7 and T9 and the removal of the spinal cord segment between the two transections, creating a 5 mm gap.

This study contained four experimental groups. Group I was the control group. The animals in this group had a complete spinal cord transection as described above but received no implantation. Group II received a resorbable dura replacement sheet of collagen, 1 mm thick, cut from the BioGide® membrane which was placed extradurally over the dorsal aspect of the wound site. Group III used the BioGide® membrane as a wrap which bridged the gap between the two cord stumps. Group IV used a collagen tube, fabricated using a freeze-drying process, to bridge the gap.

Histological analysis at 6 weeks after implantation showed Groups III and IV to have more longitudinally oriented reparative tissue filling the defect area as well as fewer fluid-filled cysts. Quantitative analysis of axonal regeneration showed the collagen implants to be supportive of the regeneration of axons into the center of the defect.

Thesis Supervisor: Myron Spector
Title: Senior Lecturer, Department of Mechanical Engineering
Professor of Orthopedic Surgery (Biomaterials), Harvard Medical School

**Acknowledgements**

My work on the spinal cord project has truly been a learning experience. Despite my limited background in the biological and biomedical fields I was able to finally bring this research together and I am grateful to my advisor, Dr. Spector, for allowing me to work on this project solely based on my heightened interest of the topic. I have learned a lot from Dr. Spector, and I appreciate his patience and enthusiasm no matter what the situation.

I would also like to thank the other members of the spinal cord regeneration team for their support and encouragement even during the times when the work could get a bit wearing like when we had to go to the animal research facility every night at midnight to express rat bladders. Dr. Hu-Ping Hsu was an invaluable resource; bringing his skills and expertise on animal surgery to the project.

On a more personal note, I would like to thank my parents for their continued love and encouragement, no matter what. Also, I thank my friends for not giving up on me despite my "disappearance" while I worked on putting this thesis together. I am truly grateful to have the friends that I do.

## Table of Contents

**List of Figures**

**List of Tables**

# Chapter 1: Introduction

## 1.1 Motivation of Research

There are currently 250,000 people in the United States who have suffered a spinal cord injury and there are approximately 11,000 new cases every year. Motor vehicle crashes account for the majority of new spinal cord injury (SCI) cases. The most common neurologic level of injury is tetraplegia (57.6% for both complete and incomplete injuries) followed by paraplegia (35.9% for both complete and incomplete injuries). Only less than 1% of patients with SCI experience full neurological recovery [1].

Patients with SCI often suffer significant reduction in quality of life. In addition to suffering paralysis and the loss of sensation below the level of injury, other basic bodily functions are often impaired including breathing, bowel and bladder control and sexual function. As a result, sufferers of spinal cord injuries lose a great deal of their independence. Additional complications that often arise with SCI are orthostatic hypotension, autonomic dysreflexia, osteoporosis, chronic pain, and pressure ulcers [2].

The financial toll that SCI imposes is quite staggering. Lifetime costs that are directly attributed to SCI vary depending on the severity of injury and are as high as $2.8 million for high tetraplegia and $900,000 for paraplegia [1].

## 1.2 The Nervous System

The nervous system is composed of a network of cells, or neurons, which are distributed throughout the body and function to transmit information as electrochemical impulses to and from and within the brain. Some of the information that is transmitted via the neural network is in response to stimuli received from both the external and internal environment of the body (sensory information), while other information transmitted by neurons is in the form of motor commands which cause muscles to contract or glands to function.

The cells of the central nervous system include neurons (which transmit information) and glia, which support neuronal function.

The nervous system is comprised of various types of neurons which reside in different parts of the nervous system. The varying types of neurons have different sizes, shapes, and functional roles. However, all neurons have a least one axon and one or more dendrites. Neurons can be categorized into three basic types. Unipolar neurons have a spherical cell body with a single process that divides into two branches (Figure 1.1A). Bipolar neurons are spindle shaped and have 2 processes (Figure 1.1B). Multipolar neurons, as their name suggests, have numerous processes coming from the cell body (Figure 1.1C) [3].

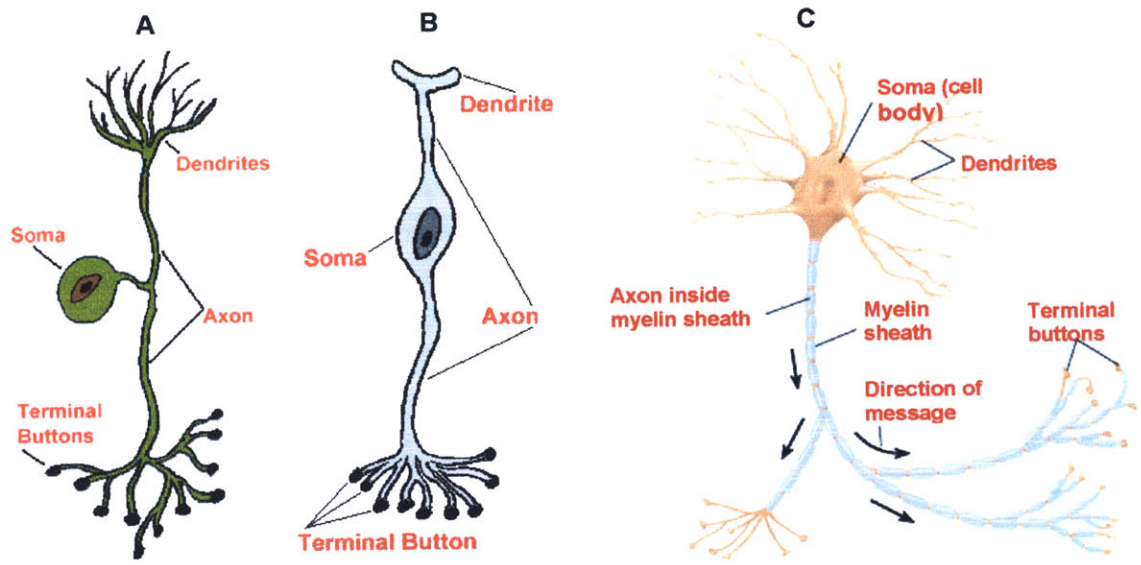


**Figure1.1** – (A) Unipolar neuron. (B) Bipolar neuron. (C) Multipolar neuron.

Key features of a neuron are the cell body - containing the nucleus and numerous organelles, the axon, and the dendrites. The axon of a neuron is connected to the cell body and departs from a location known as the axon hillock. It is the process of a neuron by which impulses are transmitted. Unlike the cell body, axons do not have any structures associated with protein synthesis or assembly. Axons vary in length, and can be up to a meter long in the spinal cord of adult humans. Axons have a cylindrical shape and can be either myelinated or unmyelinated.

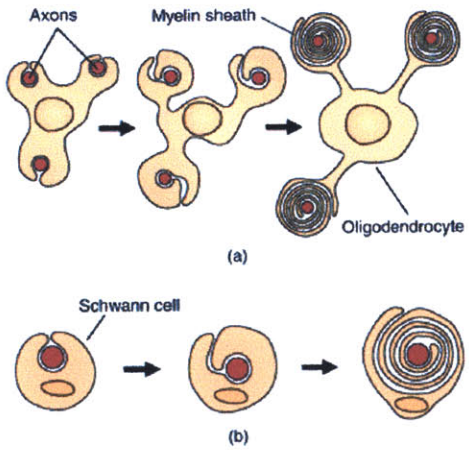


**Figure 1.2** – (a) Illustration of axon myelination by oligodendrocyte. (b) Illustration of axon myelination by Schwann cell.

Myelation occurs when axons become wrapped in multiple layers of Schwann or oligodendroglia plasmalemma (Figure 1.2). The myelin sheets serve as electric insulation to the axons and improve electrical conduction. Myelinated axons conduct nerve impulses at a faster rate than unmyelinated axons.

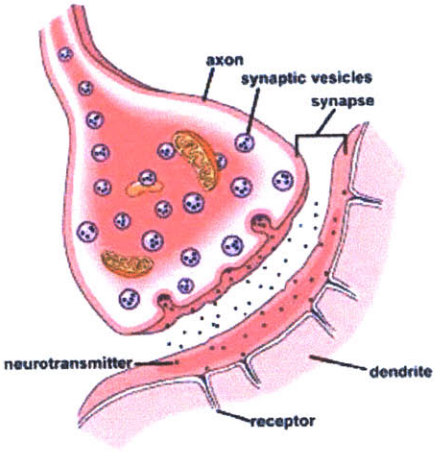


**Figure 1.3** – A neural synapse.

Another important part of a neuron is the dendrite. Dendrites contain sites for synaptic contact with axon terminals from other neurons. This site of contact between neuronal cells is called the synapse. Figure 1.3 gives an illustration of a neural synapse. The transmission across a synapse occurs through the release of neurotransmitters by the presynaptic neuron, followed by the diffusion of the molecules across the synaptic cleft, and culminating with the binding of the molecules to receptors on the postsynaptic membrane. The neurotransmitter causes a change in the permeability of the cell membrane to certain ions. For the transmission of an electric impulse the change of permeability of the membrane allows for the influx of sodium ions and the efflux of potassium ions, resulting in a localized reversal of charge of the cell membrane causing a propagation of an action potential [4]. In myelinated axons, electric impulses jump from one node of Ranvier to another. The nodes of Ranvier are the small areas of myelin discontinuity along the length of the axon. These areas of myelin discontinuity occur between the myelin coverage of one oligodendrocyte or Schwann cell and another.

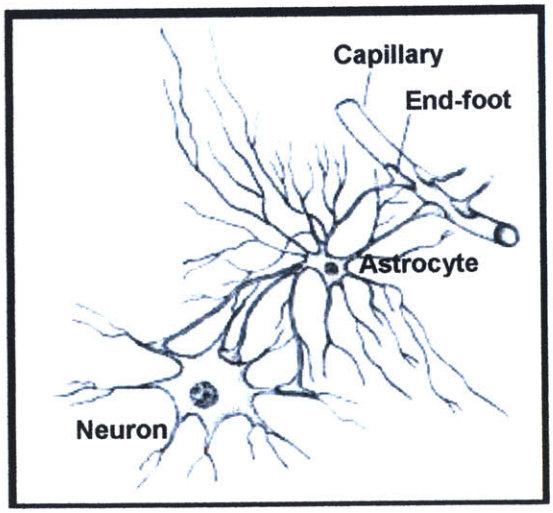


**Figure 1.4** – Astrocyte in close proximity of a neuron and capillary.

Neuroglia, the supporting cells of the nervous system, include astrocytes, oligodendrocytes and Schwann cells, ependymal cells, and microglia. Astrocytes are starlike cells and are the largest of the

neuroglia. Astrocytes have numerous processes which attach to the outer surface of capillaries. Fibrous astrocytes are involved with the repair of damaged tissue (they produce scarring) and are found primarily within the white matter. They help facilitate the metabolite transfer to neurons. Protoplasmic astrocytes are very closely associated with neurons and can partially envelop them. They are found mainly in the gray matter of the brain and spinal cord. Figure 1.4 illustrates the close association of astrocytes with neurons and capillaries.

Oligodendrocytes are commonly located among strands of axons and serve to myelinate axons. A single oligodendrocyte can myelinate numerous axons as is illustrated in Figure 1.5. Oligodendrocytes can be found in both the grey and white matter.

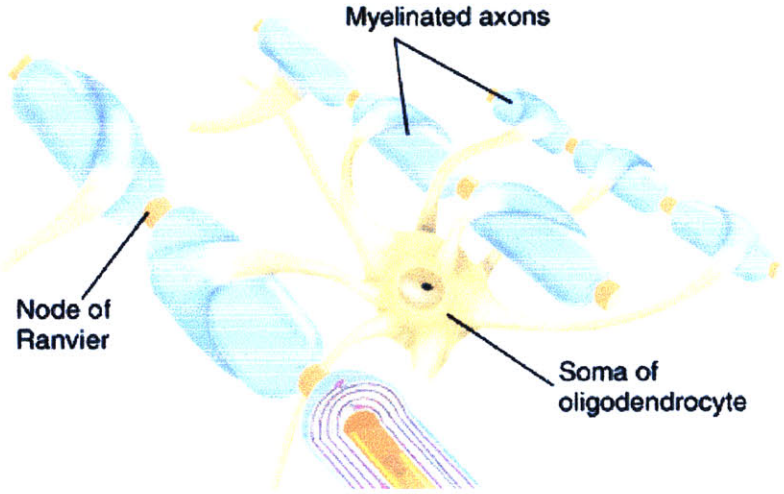


**Figure 1.5** – Oligodendrocyte.

Schwann cells are the counterparts to oligodendrocytes in the peripheral nervous system. A single schwann cell can myelinate a short segment of a single axon.

Ependymal cells line the central canal of the spinal cord and the ventricles of the brain and are responsible for the production of cerebrospinal fluid.

Microglia, on the other hand, are of mesodermal origin and play the role of immune cells for the central nervous system. These cells are phagocytic and respond to disturbances of the nervous system.

## 1.3 The Spinal Cord

The spinal cord functions as the integral link between the brain and the peripheral nervous system. It is protected by the spinal vertebrae (Figure 1.6A), meninges and cerebrospinal fluid [5]. There are three meninges which surround the spinal cord. They are the pia mater, arachnoid and the dura mater (Figure 1.6B). The dura mater is the thickest of the three meninges.

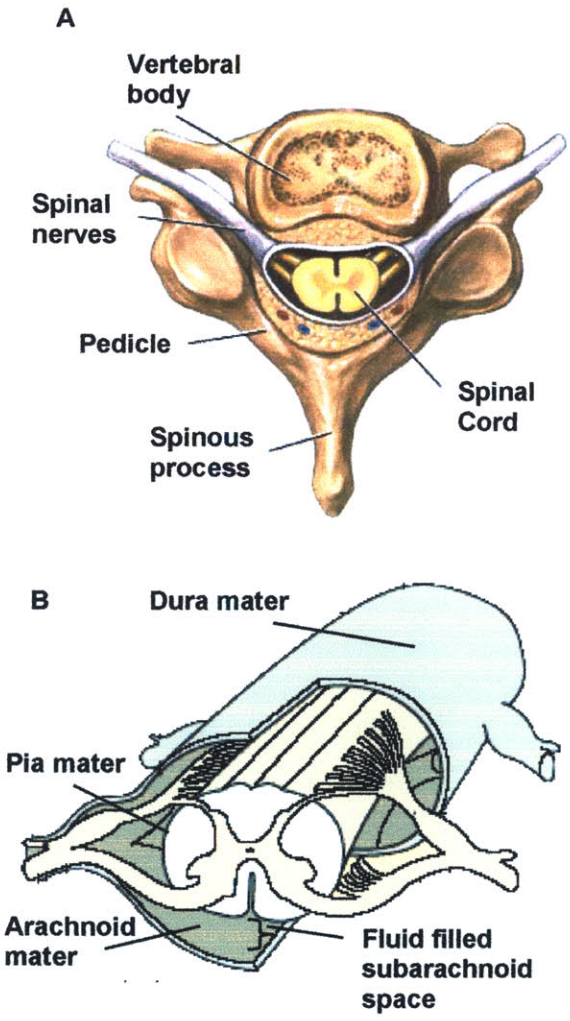


**Figure 1.6** – (A) Cross-sectional view of the spinal cord within the vertebra. (B) Illustration of the spinal cord with surrounding meninges

The two distinct regions of the spinal cord cross-section are the grey and white matter (see Figure 1.7). The grey matter is centrally located and has a butterfly shape. It is composed primarily of neuronal and glial cell bodies. The dorsal horn of the gray matter is where the dorsal roots are received. The ventral horn of the gray matter is comprised primarily of multipolar motor neurons the axons of which form the ventral roots. The white matter, on the other hand, is composed primarily of descending and ascending axonal tracts. Axons with common function, origin and destination are found within particular tracts (see Figure 1.7). The central and peripheral nervous systems are bridged by means of the dorsal and ventral roots. The dorsal roots carry sensory signals from the peripheral nervous system to the central nervous system while the ventral roots contain motor axons that relay motor

commands from the central nervous system to the muscles through the peripheral nervous system.

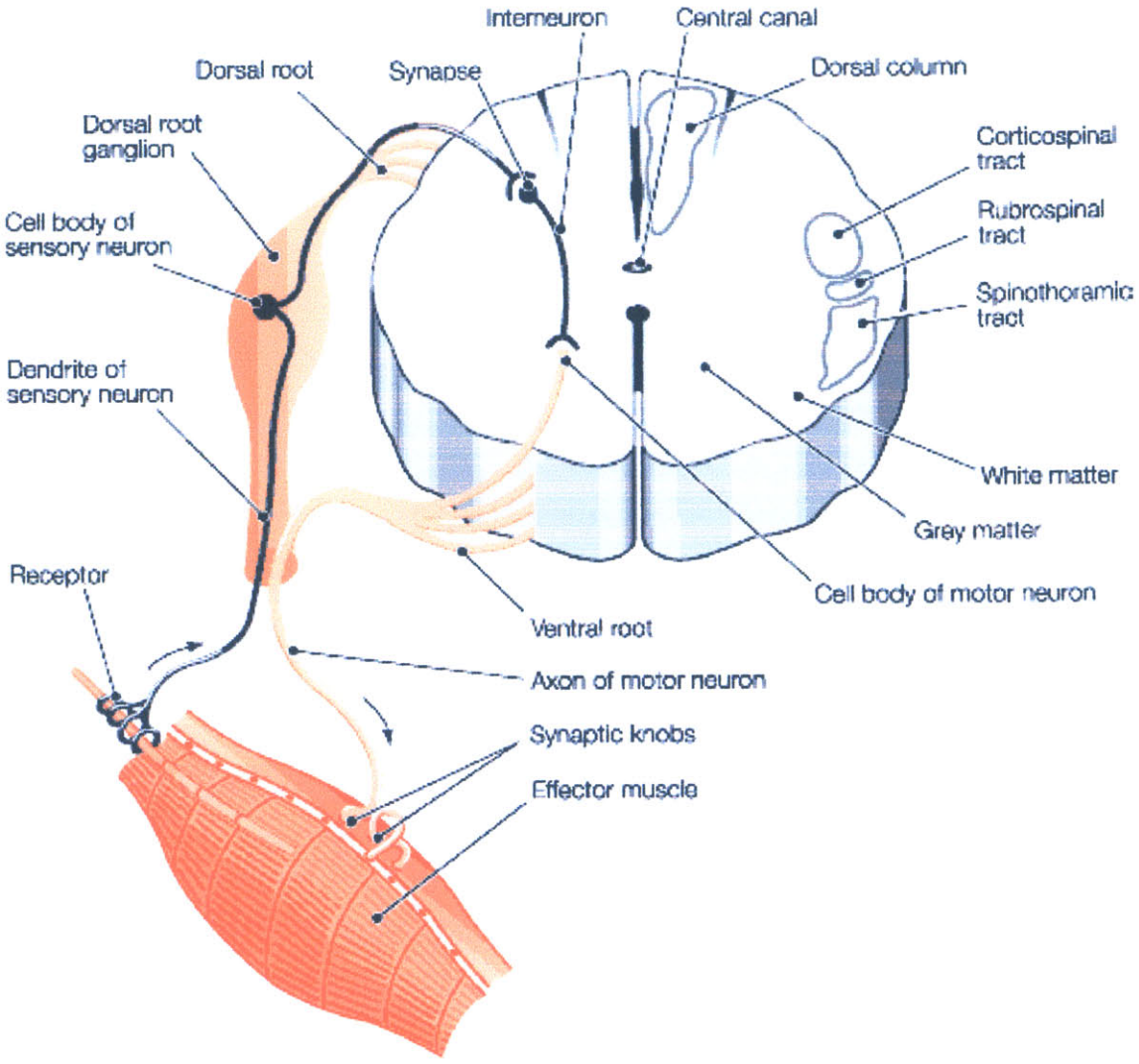


**Figure 1.7** – The spinal cord cross-section showing the gray and white matter, dorsal and ventral roots, various axonal tracts and a synapse for a spinal cord mediated reflex.

Some sensory inputs to the peripheral nervous system are responded to via spinal cord mediated reflexes. This means that a sensory input (such as a pin prick) could be responded to (i.e. muscle contraction) without the signal being relayed to the brain. This is illustrated in Figure 1.7 by the synapse and interneuron connected within the gray matter.

Each segment of the spine has a corresponding pair of dorsal and ventral roots. These roots innervate specific areas of the body. Dorsal and ventral roots stemming from

a specific segment of the spine generally innervate areas of the body at the same level as the particular spinal segment. This is illustrated in Figure 1.8.

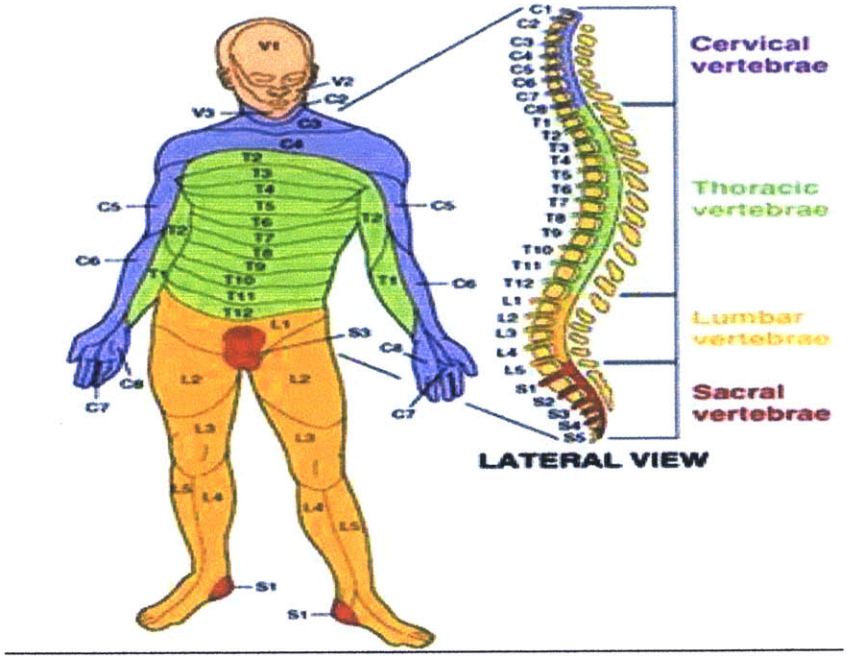


**Figure 1.8** – Areas on the human body and the corresponding spinal root locations for innervation.

The spinal cord is highly vascularized. It receives blood supply from one anterior and two posterior spinal arteries. These arteries run longitudinally throughout the length of the spinal cord. Venous drainage of the cord is carried out by three anterior and three posterior spinal veins (Figure 1.9).

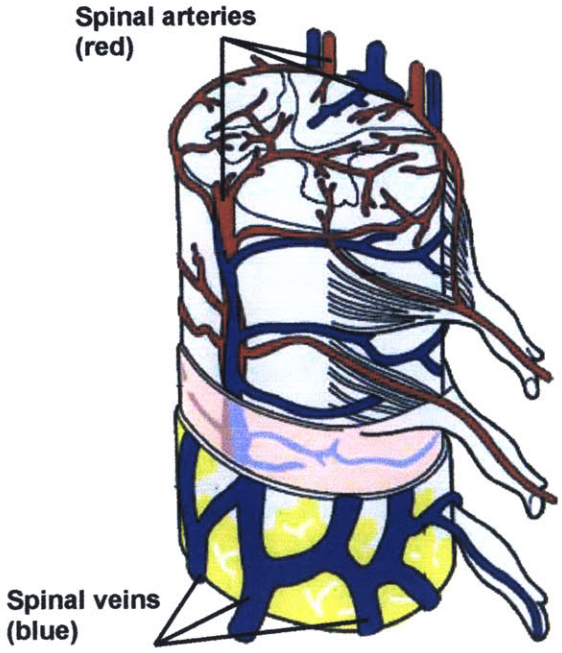


**Figure 1.9** – Vasculature of the spinal cord

### 1.4 Normal Injury Response of the Peripheral Nervous System

When an axon in the peripheral nervous system is injured, degeneration occurs both proximal (closer to the cell

nucleus) and distal to the injury location. Initially, there is an influx of sodium and calcium at the injury site and a significant loss of potassium and protein. The proximal degeneration generally occurs only over a short distance. Axonal sprouting from the proximal stump begins within a short time but axonal debris and scaring may fill the defect and prevent proximal growth cones from reaching the distal stump. Distal degeneration is characterized by Wallerian degeneration. The axon begins to degrade while macrophages invade and remove remaining axonal debris from the Schwann cell sheaths. Eventually, myelin sheaths begin to undergo disintegration and macrophages are thought to be involved with the removal of the myelin debris as well. An endoneurial tube is left along the entire length of the degenerated axon. If the injury gap is small enough, an axon sprout may find a distal tube and continue to grow in length and diameter until it eventually re-innervates its target while remaining sprouts from the proximal axon stump degenerate. Neuroma may develop if the axon sprouts do not find the distal tubular pathways. Also, if a sensory axon finds a distal tubular pathway of a motor neuron or vice versa, the axon will not be functional [4]. Figure 1.10 illustrates the process of peripheral nerve regeneration.

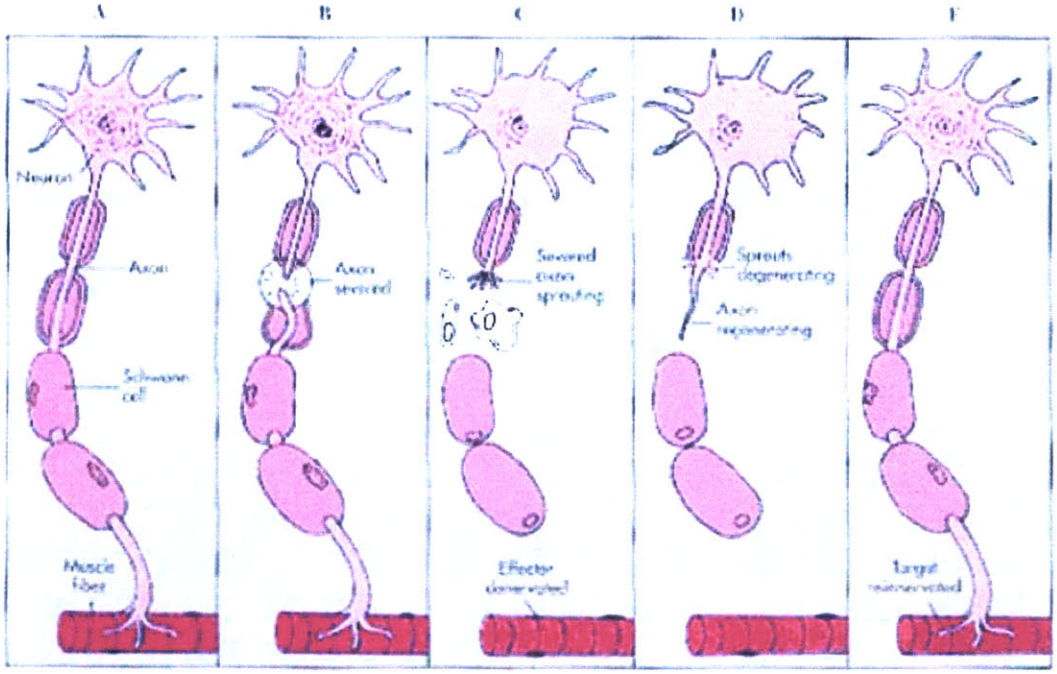


**Figure 1.10** – (A) An uninjured neuron. (B) The axon is severed and Wallerian degeneration begins. (C) Axonal sprouting occurs from the proximal stump. Macrophages remove debris. (D) Axon begins regenerating. (E) Regenerating axon finds target.

### 1.5 Normal Injury Response of the Spinal Cord

Injury to the spinal cord results in two distinct modes of tissue damage. The first is acute tissue damage which results directly form the disruption of the tissue and causes extensive cell death at the injury site. The second mode of tissue damage, or secondary tissue damage, is tissue degeneration that continues well after the initial injury. Secondary damage occurs as a result of various events which occur is response to the acute injury. Immediately following the initial injury, there is considerable hemorrhaging that takes place and affects the normal oxygen and nutrient supply to the affected tissue. The body then responds to the acute injury with a strong inflammatory response which leads to edema of the spinal tissue. As this occurs, neural cells begin to die and release excitotoxins such as glutamate which causes further neural cell death [6]. Another adverse occurrence is the formation of free radicals which cause extended damage to surrounding nervous tissue. The unfavorable conditions are heightened by the demyelization of remaining axons due to the loss of oligodendrocytes. As spinal tissue is lost and removed by phagocytes, fluid-filled cysts are formed within the lesion. Dense fibrous and glial scar formation occurs at the injury site which impedes any attempts of the axons to spontaneously regenerate across the defect. Reactive astrocytes, which form the glial scar, express chondroitin sulphate proteoglycans, which inhibit axonal growth. Other inhibitory molecules are found in the degenerating myelin including NOGO-A, MAG, and OMpg [7]. In response to being severed, the distal segments of damaged axons undergo Wallerian degeneration while the proximal segments retract away from the injury site.

The rather hostile environment ensuing injury to the spinal cord impedes the spontaneous regenerative processes, including axonal sprouting, that occur following nerve damage.

### 1.6 Current Clinical Treatments of SCI and Ongoing Research

The emphasis of the initial treatment of a spinal injury is on immobilization of the spinal column to prevent further nerve damage. Surgical intervention is commonly required to provide realignment and stabilization of the spine and decompression of the spinal cord. The intravenous administration of methylprednisolone in high dosages

within 8 hours of injury was reported by Bracken et al. to significantly reduce the effect of secondary injury in a multicenter randomized clinical trial. Methylprednisolone was reported to be of benefit only if administered within the 8 hour period following spinal cord injury [8]. Despite the broad acceptance of methylprednisolone as a clinical treatment for SCI there is still considerable controversy over the efficacy of this steroid treatment [9]. To date there are no clinical therapies which actively promote the regeneration of the damaged nervous tissue.

Many experimental SCI treatment strategies are being investigated in animal models and reported in the literature with varying degrees of promise. Some approaches to spinal cord regeneration involve development and evaluation of various substrates to provide guidance and act as a bridge to axonal growth across a defect in the spinal cord [10-12]. The focus of some studies is the ability of certain neurotrophic factors and gene therapy strategies for creating favorable conditions for axonal growth. Other studies have looked at the implantation of various cell types into the damaged spinal cord to replace lost cells and facilitate nerve repair [14]. Various stem cell approaches have been studied, including the implantation of neural stem and progenitor cells into spinal cord lesions [15]. In many studies the implanted cells are first genetically encoded to express specific neurotrophic factors [16]. Bone marrow mesenchymal stem cells implanted into damaged spinal cords of adult rats have been reported to simulate nerve regeneration [17-20]. Lu et al. reported that BDNF-expressing marrow stromal cells supported axonal regeneration in adult rats [21]. Furthermore, olfactory ensheathing glia have been reported to promote long distance axonal growth when implanted into the defect of a transected rat spinal cord [22-24]. In another study, neurotrophin-3 (NT-3) expressing olfactory ensheathing glia cells were reported to promote spinal sparing and regeneration in adult rats [25]. While some researchers only implant cells into the spinal cord lesion others implant them in combination with a biomaterial scaffold [26-28]. The identification of inhibitors to regeneration (such as NOGO-A) and the application of agents to block or overcome these inhibitors has shown promise in improving axon recovery after spinal cord injury [7, 29-31]. In one study, the use of an oscillating field stimulator, which produced an electric field across a lesion in the spinal cord, was shown

to induce limited sensory recovery and improve motor function in patients participating in a phase 1 clinical trial [32].

Previous work in our laboratory has shown the effectiveness of collagen tubes in promoting axonal regeneration across significant gaps in the rat peripheral nerve [33, 34]. The tubes performed better than the nerve autograft "gold standard". Our laboratory has also investigated the use of collagen tubes for spinal cord regeneration. Results showed that tubulation of a transected adult rat spinal cord had beneficial effects on spinal cord healing such as a reduction in scar formation and improved axonal and connective tissue orientation within the defect [35, 36]. This past work forms the basis for the current hypothesis that collagen based implants have beneficial effects on spinal cord regeneration.

Notwithstanding the encouraging results for spinal cord regeneration that many researchers have reported in the literature, there has yet to be a single therapy which can provide satisfactory recovery from traumatic spinal cord injury. It is likely that an effective treatment for spinal cord injury will require a multifaceted approach to nerve regeneration; combining various spinal cord regeneration strategies.

### 1.7 Aim of Research Project and Specific Goals of this Thesis

The long term objective of this research project is the development of an implant for the treatment of spinal cord injuries in humans. The implant will likely make use of a combination of therapies shown to support regeneration of the spinal cord. The therapies currently investigated include porous, structurally aligned, bioresorbable collagen scaffolds, stem cell therapies, inhibitor blocking antibodies, and the use of neurotrophic factors delivered via scaffold binding and/or cellular transfection.

The specific aim of this thesis is to compare select collagen implants for their abilities to promote axon regeneration in the adult rat spinal cord. The goal is to find an optimal entubulation strategy which can be used in the future in combination with the spinal cord regeneration therapies mention above. The primary method for the evaluation of the efficacy of the various implants will be qualitative histology and quantitative axonal regeneration analysis.

The BioGide® sheets were prepared into a slurry suspension (5% w/w) by cutting them into small pieces (1 $mm^2$) then mixing with a 0.5 M acetic acid solution. The collagen slurry was thoroughly mixed until a homogenous mixture was achieved. A 10-ml syringe containing the collagen slurry was attached to another 10-ml syringe with a Luer-lock assembly, and mixed by injecting collagen slurry from one syringe into the other (approximately 30-40 times) until the collagen fibers began to hydrate and the solution appeared uniform.

After letting the slurry sit for 3 hours at room temperature to allow for the collagen fibers to swell, the collagen slurry was centrifuged in order to de-gas the collagen so that any macroscopic air bubbles were removed from the slurry.

During centrifugation the slurry tended to separate into two phases. In order to re-homogenize the slurry, it was gently mixed using the syringes and Luer-lock assembly 2-3 times very slowly taking care not to allow any air to be mixed into the solution.

The collagen slurry was injected into the Teflon mold. The slurry (~0.8 ml per tube) was injected into one side of a channel in the closed mold until it started to come out of the other side of the channel. The glass rod with its silicone sheath was then inserted into the channel which had been filled with slurry. The rod was rotated during its insertion so as to keep the rod centered in the channel and to maintain a uniform coverage of the rod with the collagen slurry throughout the channel. When the rod came out of the other side of the channel, a centering ring/spacer was slipped over the rod. This procedure was repeated for each of the 6 channels in the mold.

The mold was placed into a freeze-drier (set to -40°C) for 1 hour. After freezing, the mold was removed from the freeze-drier and quickly split open, in order for the frozen collagen tube to be gently removed from the mold. The glass/silicone rods were kept inside of the collagen tubes. The tubes with the rods in place were inserted back into the freeze-drier (at -40°C).

A vacuum below 100 mTorr (taking ~30-60 minutes to reach) was applied to the freeze-drier. The temperature was then raised to 0°C and the samples left overnight under vacuum in the freeze-drier (17 hours). The temperature was subsequently raised to 20°C and the vacuum released.

implant a device for facilitating axonal regeneration. Unilateral hemesectional models offer the advantage of being able to assess an implanted device while still preserving the structural integrity and function of one side of the spinal cord [26].

For this study the complete transection model was chosen as it offers the best method for evaluating the effects of an implanted device on axonal regeneration.

### 2.3 Animal Model

The most common animal model used for spinal cord injury research is the adult rat. For this reason there is an abundance of data in the literature that allows for easy comparison of result from different studies. Compared to other animals, rats are inexpensive, can be studied in large numbers, require less intensive post operative care, and have relatively low mortality rates. Transgenic mice offer the researcher the distinctive ability to control particular genetic characteristics; however, the small size of mice may prohibit certain surgical procedures and device implantations [37].

Larger animal models such as cats, dogs, pigs and primates are not used as widely in the literature. These animal models are less attractive due to the higher cost and more intensive animal care; however, using a large animal model may be important before performing trials on humans.

In this study, the rat was chosen as the animal model for the reasons mention above and also due to the fact that our laboratory has extensive experience in using rats for both peripheral nerve and spinal cord regeneration studies [13, 33-36, 39, 40].

Female rats were used in this study because they allow for easier management of the loss of reflex bladder control following spinal cord transection. The loss of bladder function necessitates the manual expression of urine from the bladders of the rats following complete spinal cord transection. Using female rats facilitates the manual expression of the bladder.

### 2.4 Rat Strain Choice

The first three experimental groups in this study used Sprague-Dawley (SD) rats weighing between 250 to 300 grams. There was an approximately 40% incidence of self-mutilation in the SD rats, most commonly in the form of extreme biting of the skin of the

## Chapter 2: Methods and Materials

### 2.1 Collagen implants

The collagen implants used include a collagen tube and a collagen sheet.

### 2.1.1 Tube Fabrication Materials

Collagen tubes were fabricated from a slurry prepared from BioGide® sheets composed of types I/III collagen. The protocol used is a modification of the method previously used for making tubes in our laboratory from bovine collagen and reported in the literature [13].

A mold was used to form the collagen tubes out of the collagen slurry. Polytetrafluoroethylene (Teflon) was used to make the mold, which contained six channels, each 5 mm in diameter, drilled through the Teflon. The Teflon mold is contained within an aluminum housing to provide rigidity (see Figures 2.1 and 2.2).


**Figure 2.1** – Mold used for fabricating collagen tubes.

The collagen tubes (with the glass/Teflon rods in place) were removed from the freeze-drier and placed into aluminum foil bags for storage.

Collagen tubes were dehydrothermally crosslinked flowing the freeze-drying process. The tubes were placed in a vacuum oven for 24 hours at 105° C. This step also served the purpose of sterilization of the tubes. The detailed protocol for dehydrothermal treatment is in Appendix A.

The tubes fabricated using the above technique had the following dimensions: inner diameter of 2.95-3.0 mm and outer diameter of 4.7-4.8 mm. A picture of a tube is shown in Figure 2.4.

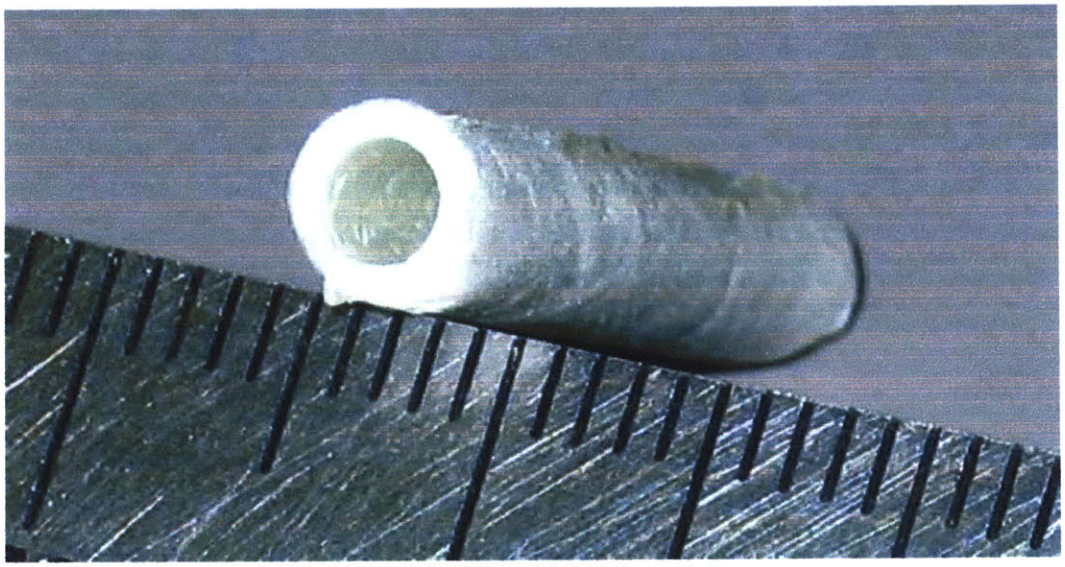

**Figure 2.4** – Collagen tube (scale is mm).

### 2.1.2 BioGide® Membrane

The BioGide® (Geistlich Biomaterials, Wolhusen, Switzerland) sheet is a collagen type I/III membrane that is commercially available in the US and in many European countries. Its primary use is in certain dental and maxillofacial procedures. The membrane has a bilayer design which combines 2 distinct layers to form the membrane. One is a smooth dense layer which is less permeable while the second is a porous layer which favors tissue integration. Figure 2.5 shows the microstructure of the BioGide® membrane (taken from the Geistlich Biomaterials website).

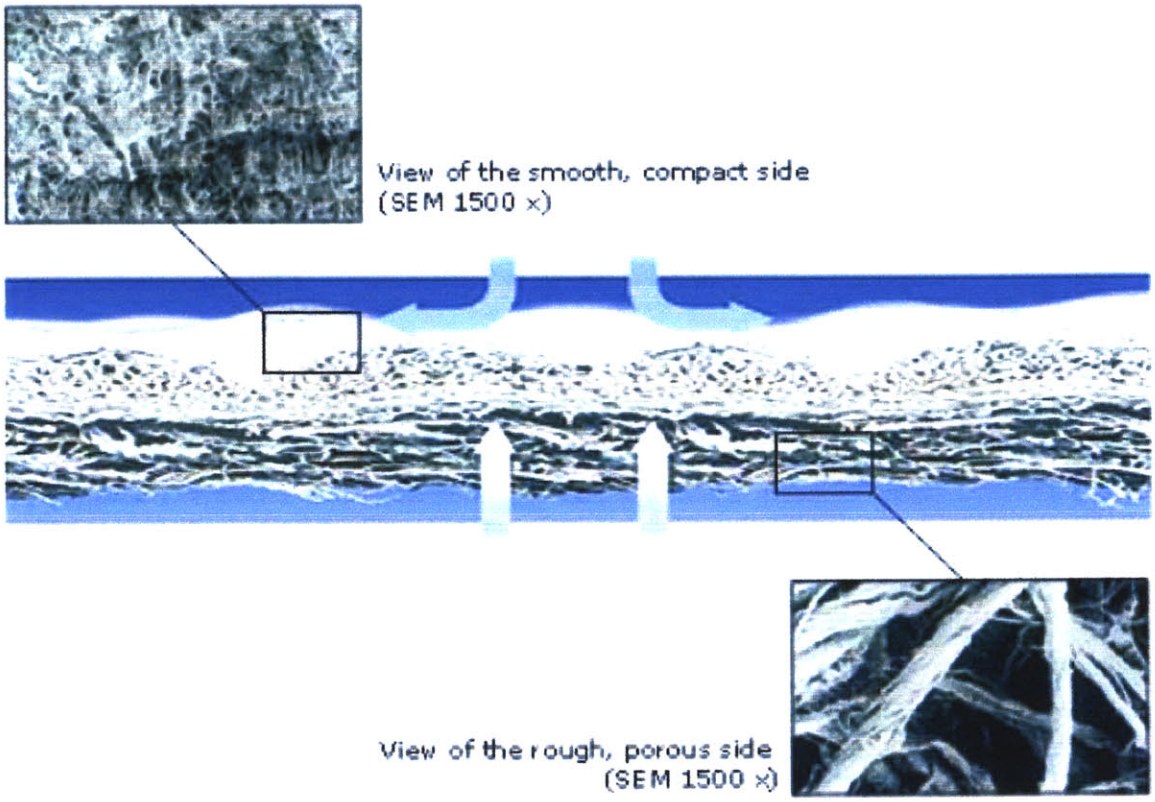


**Figure 2.5** – Illustration of the microstructure of the BioGide® membrane.

## 2.2 Spinal Cord Injury Model

There are a wide variety of injury models that are used in spinal cord injury research. Contusion and compression models are often chosen as they more closely parallel SCI seen in the clinic. These models may be better suited for studies which investigate treatments designed to manage the onset of secondary tissue damage [37]. Experimental contusion injuries are often created by using a computer controlled impactor or a weight drop device which drops a weight on the exposed spinal cord [18, 19, 38]. Experimental compression injuries are often created by applying a surgical spring-loaded clip or a balloon which applies pressure on the spinal cord. Complete transection models fully sever the spinal cord. This approach has the advantage of being able to unambiguously demonstrate the regeneration of axons into the lesion; something that would be difficult with a contusion model since it is not easy to distinguish between spared and regenerated axons. Another advantage of a transection model is the ability to

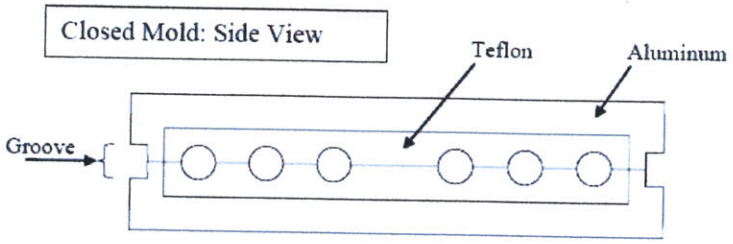


**Figure 2.2** – Side view of closed mold.

Glass rods were used to form the lumen of the tubes and were contained within a silicone sheath. Each glass rod was 2.5 mm in diameter (measured 2.46-2.48 mm). The silicone tubing fitted over the glass rod had an inside diameter of 2.5 mm and an outside diameter of 3.0 mm.

In order to center the rod in the middle of the channel, a Teflon spacer was inserted over the end of the rod as it came out either end of the channel (*i.e.*, 2 Teflon spacers per rod). The Teflon spacers have an inside diameter of 3.0 mm and an outside diameter of 5 mm. The nominal inner diameter of a tube prepared in the mold was 3 mm; the outer diameter was 5 mm. Figure 2.3 shows the glass rod with a silicone sheath and Teflon spacers.

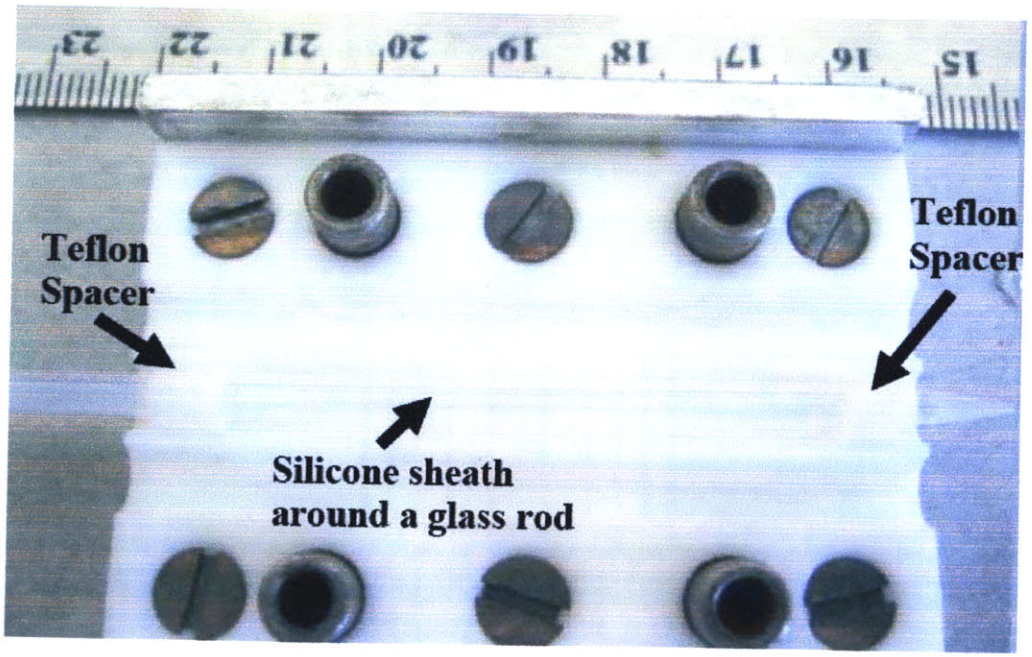


**Figure 2.3** – View of the glass rod with a silicone sheath and Teflon spacers in the open mold.

### 2.1.2 Tube Fabrication Protocol

abdomen. In many cases, the self-mutilating animals had to be euthanized due to the severity of the lesions. This prompted the investigation of the use of an alternative rat strain. In the literature it is reported that Lewis rats alone do not exhibit self-mutilation following sciatic nerve injury [41, 42]. However, there has been no clear comparison for spinal cord work. Because of the notable difference in the rates of self-mutilation of Lewis rats compared to other rat strains for peripheral nerve injuries, it was hypothesized that a similar reduction in incidence of self-mutilation would be seen for spinal cord injuries. One disadvantage of the Lewis rat is its smaller size which increases the difficulty of the surgical implantation. Adult Lewis rats are about 40% smaller than adult SD rats. Notwithstanding this drawback, a switch to using Lewis rats was made in order to reduce the rates of self-mutilation. In our experience to date with the Lewis rats, we have not had any cases of self-mutilation.

**2.5 Rat Surgery**

Adult female Sprague Dawley (groups I-III) or Lewis rats (group IV) (Taconic, Germantown, NY) weighing 250-300 and 150-175 grams respectively were used in this study. All animal care and surgical procedures were performed at the Veterans Administration Medical Center Animal Research Facility (Jamaica Plain, MA). All surgical and post-operative procedures were approved by the VA Boston Healthcare System Institutional Animal Care and Use Committee (IACUC).

Rats were anesthetized by an intraperitoneal injection with sodium pentobarbital (Nembutal solution, 50 mg/ml, Abbott Laboratories, North Chicago, IL) at a dosage of 45 mg/kg. The hair on the back of the anesthetized rat was shaved and the skin was cleaned with Betadine. Surgery was performed under sterile conditions. A continuous oxygen supply was supplied to the rat during surgery. The rat was placed on a flat operating board in a prone position and the rat's limbs were gently constrained with rubber bands in an extended position. A longitudinal incision, 2 inches in length, was made through the skin above the thoracic spine. The back musculature was incised along the midline and dissected away from the vertebral column. A dorsal laminectomy was performed between T7 and T10 using small bone rongeurs and microscissors. The dura was opened with a surgical blade to expose about 10 mm of spinal cord (Figure 2.6 -

left). Two spinal cord segments (T8 and T9) were removed by performing two complete transections and removing the intervening tissue. This resulted in a 5 mm long gap in the spinal cord (Figure 2.6- right). The nearest pair of spinal roots entering the intact rostral (T7) and caudal (T10) spinal cord was severed. Gelfoam was temporarily placed in the gap to induce hemostasis.

**Figure 2.6** – Left: 10 mm section of exposed spinal cord. Right: 5 mm gap created in thoracic spinal cord

This thesis will report on 4 experimental groups. Group I (n = 8) is a control group. The animals in this group had a complete spinal cord transection as described above but received no implantation (Figure 2.7A). Group II (n = 7) received a resorbable dura replacement sheet of collagen, 1 mm thick, cut from the BioGide® membrane which was placed extradurally over the dorsal aspect of the wound site and extended 2 mm past the spinal cord stumps on both sides of the defect (Figure 2.7B). Group III (n = 4) used the BioGide® membrane as a wrap which bridged the two stumps by tucking the BioGide® membrane under the stumps then folding the sides of the sheet over the top of the defect to enclose the gap (Figure 2.7C). Group IV (n = 7) used the collagen tube, which was split open with a single cut along the long axis of the tube immediately prior to implantation, allowing for easier insertion of the ends of the cord into the tube (Figure 2.7D). After the stumps of the cord were inserted into the tube the tube automatically recovered its original shape, bringing the split ends together. As a result, sutures were not necessary to keep the tube closed. All implants were briefly hydrated in sterile saline

prior to implantation. Tubular implants were carefully filled with sterile saline to remove air bubbles within the tubes.

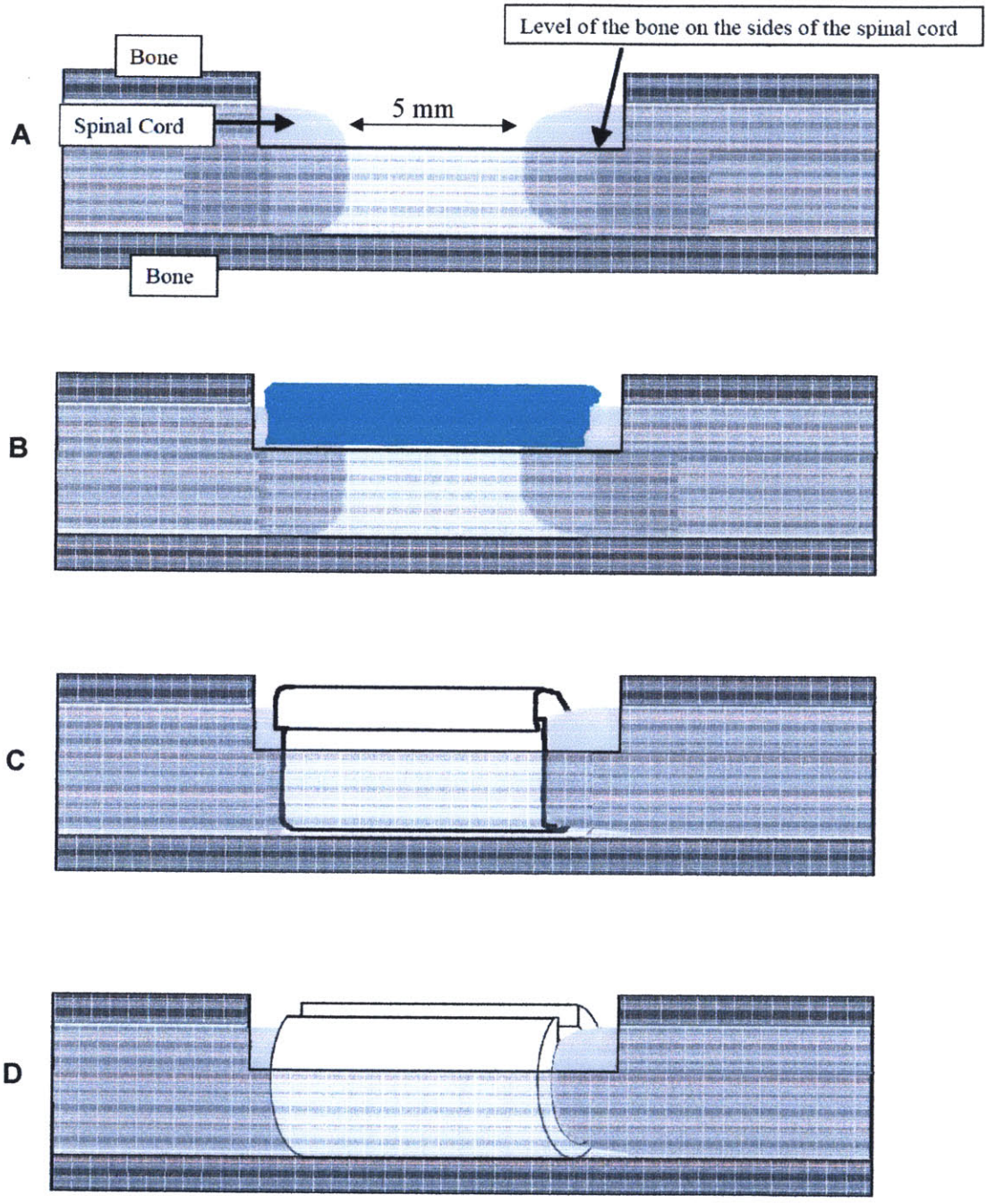


**Figure 2.7** – (A) Group I: Control, no implantation. (B) Group II: BioGide® collagen membrane used as a dorsal barrier. (C) Group III: BioGide® collagen membrane used as a wrap. (D) Group IV: Collagen tube spilt longitudinally and tucked under spinal cord stumps.

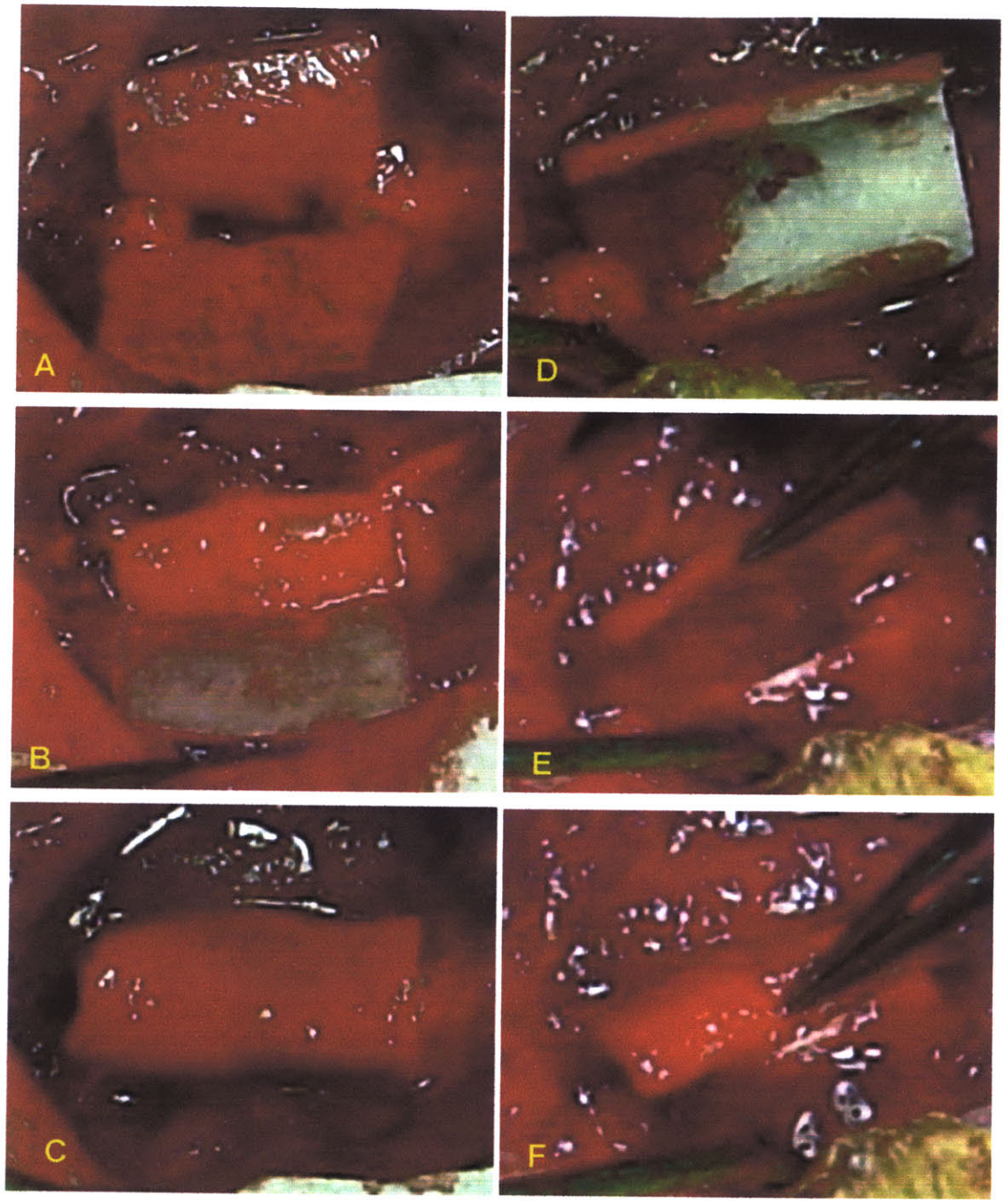


**Figure 2.8** – (A-C) The wrapping of the spinal cord stumps using the collagen membrane for Group III animals. (D-F) The bridging of the spinal cord stumps using the collagen tube for Group IV animals.

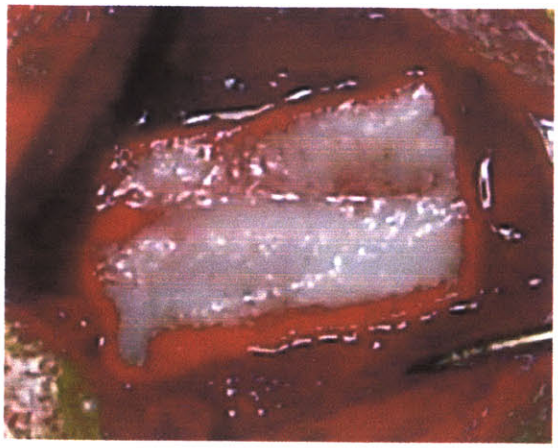

**Figure 2.9** – The collagen membrane placed over the defect area for Group II animals.

Following placement of the respective implants, the overlying musculature was closed with 4-0 vicryl sutures (Johnson and Johnson, Sommerville, NJ) and the skin was closed with wound clips.

Immediate post operative care of the animals included placement of the rat on a heating pad to maintain body temperature, subcutaneous injection of 1-2 ml of lactated Ringer's solution to compensate for blood loss during surgery, subcutaneous injection of antibiotics (cefazolin sodium 100 mg, Abbot Laboratories, North Chicago, IL), and a continuous supply of oxygen until the animal regained consciousness 4-6 hours later (Figure 2.10). After regaining consciousness, the rats were transferred to plastic cages with fresh wood chip bedding and free access to food and water. An analgesic, buprunorphine (Buprenex 0.3 mg/ml), was administered every 12 hours for 4 days following surgery by intramuscular injection into a hind leg of the animal at a dosage of 0.1 ml and 0.06 ml for the SD and Lewis rats respectively. Subcutaneous injection of lactated Ringer's solution (2 ml per day) was continued for 4 days following surgery to prevent dehydration. Administration of antibiotics (cefazolin sodium) was continued for 2 weeks, to prevent bladder infection, at a dosage of 0.15 ml and 0.09 ml per day for SD and Lewis rats respectively. Post-operatively, animals lacked normal micturition reflex

**Figure 2.10** – Rat post-operative care.

and their bladders had to be emptied manually every 12 hours using Crede's maneuver. The SD rats recovered spontaneous voiding ability after 2-3 weeks at which point manual bladder expression was stopped; however, the Lewis rats did not recover spontaneous voiding ability during the length of this study (6 weeks).

### 2.6 Spinal Tissue Removal

Six weeks post surgery the rats were sacrificed by carbon dioxide inhalation. Immediately following sacrifice, the skin covering the spinal column was incised and the site of spinal cord injury was located. The thoracic spinal column was removed using a scalpel and surgical scissors. The steps are shown in Figure 2.11. The extracted spine was placed in 10% buffered formalin at 4°C for a minimum of 72 hours.

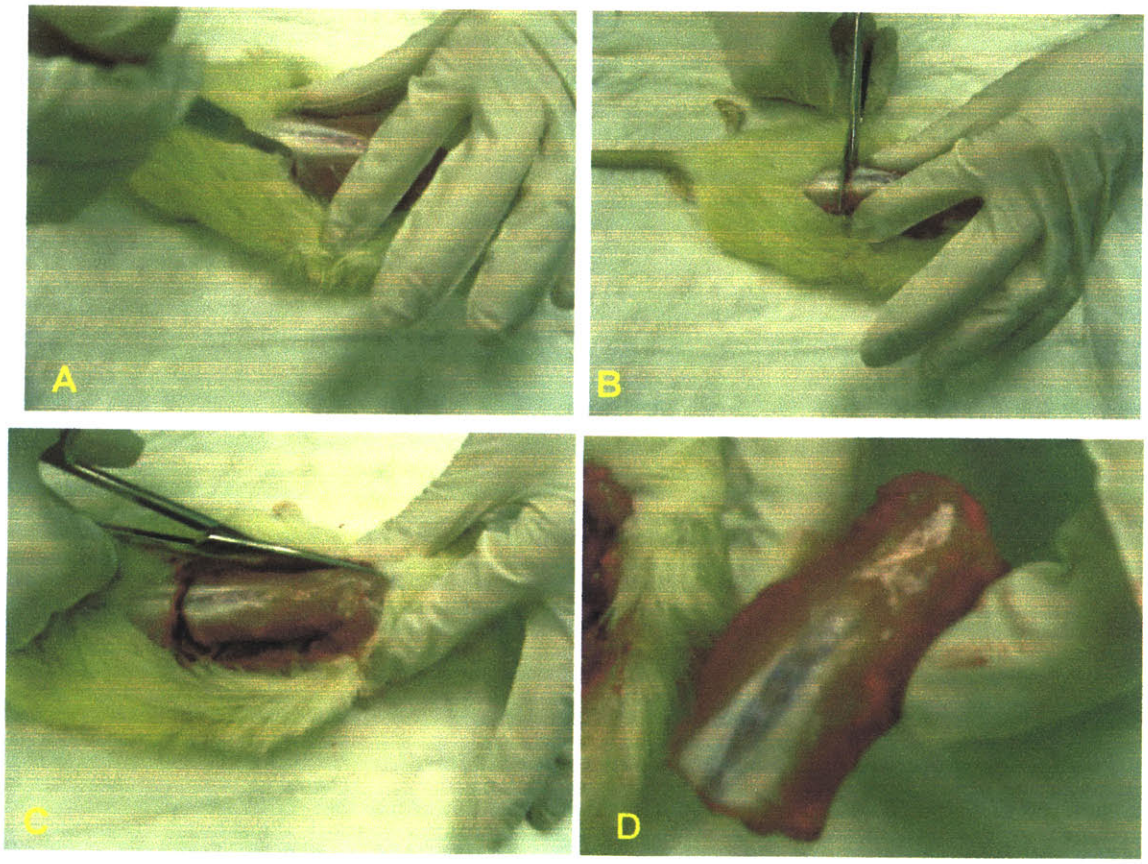


**Figure 2.11** – Steps for the extraction of the thoracic spinal column.

The intact spinal cord (2.12), including the defect area, was removed from the extracted vertebral column using bone ronguers and fine surgical scissors. The defect could be

located during the spinal cord extraction process due to the absence of the dorsal aspects of the T7 through T10 vertebrae which underwent laminectomy during the spinal surgery. The extracted spinal cord was then cut at the center of the defect using a No.11 surgical blade creating two spinal cord segments; one rostral to the defect-center and one caudal to the defect-center.

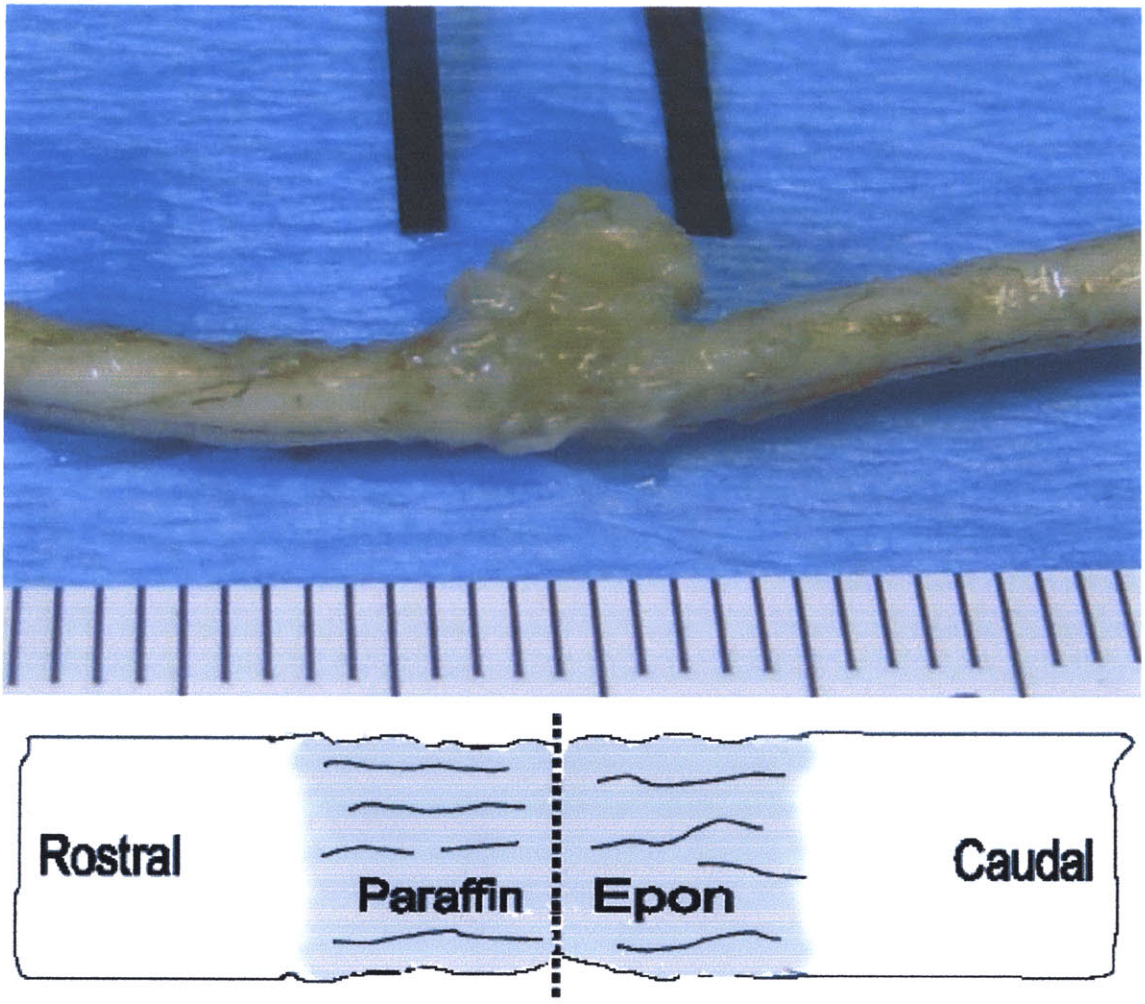


**Figure 2.12 – Top**: Image of extracted spinal cord (scale marks are mm). Black bars indicate location of lesion. **Bottom**: Illustration of the sections of the extracted spinal cord to be embedded in Paraffin (wax) and Epon (plastic).

## 2.7 Histology

### 2.7.1 Plastic Embedded Specimen

The spinal cord segment rostral to the defect-center was embedded in epon (plastic) using a Poly/Bed 812 Embedding Kit (Catalog No. 08792, Polysciences, Inc., Warrington, PA). The detailed embedding protocol is shown in Appendix B. Prior to embedding the specimen was post-fixed in 1% osmium tetroxide to stain for myelin. Plastic embedded specimens were mounted onto an ultramicrotome and 1 μm thick sections were cut to capture the cross-sectional area of the defect-center. Plastic sections containing spinal tissue were stained with toluidine blue, to provide better contrast for light microscopy analysis, and then mounted on glass slides and coverslipped. Figure 2.13 shows a plastic embedded specimen.

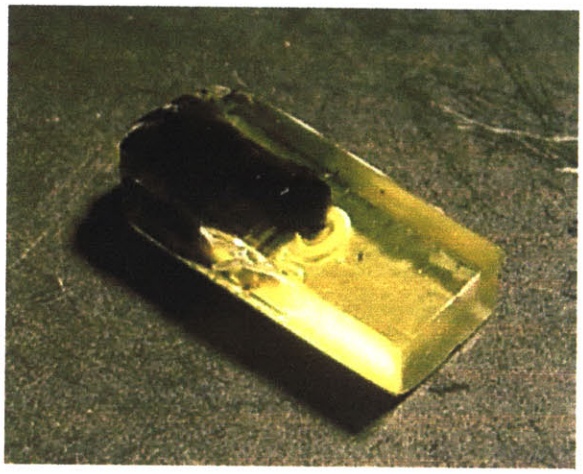

**Figure 2.13** – Image of plastic embedded spinal cord section

### 2.7.2 Wax Embedded Specimen

The spinal cord segment caudal to the defect-center was embedded in paraffin using a tissue processor (HypercenterXP, Tissue Processor, ThermoShandon, Houston, TX). Longitudinal sections of the defect were cut at 6 μm with a microtome, mounted on glass slides and coverslipped.

Adjacent tissue sections were stained with hematoxylin and eosin (H & E) for general observation of cellular and extracellular matrix features and Masson's trichrome which was used to identify the presence of collagenous tissue within the defect. The protocols used for these staining methods are listed in Appendix C.

### 2.7.3 Method for the Quantitative Analysis of Axonal Regeneration

Plastic embedded cross-sections of the defect-center which were stained with osmium tetroxide and toluidine blue were examined using a light microscope outfitted with a digital camera. Images of the defect-center were captured first at low magnification (40x) in order to view the entire lesion cross-section (Figure 2.14A). Additional images were captured at 200x magnification to provide sufficient resolution

for the identification of individual axons (Figure 2.14B). The images were opened in Adobe Photoshop and were converted to black and white; then the brightness and contrast were increased until the axons were clearly outlined (Figure 2.14C).

The black and white images were analyzed using ImageJ software (available as freeware from NIH, Bethesda, MD). This software can be utilized to measure various parameters in the histological section including: the total number of axons, the area of each individual axon, the average axonal area and standard deviation, the percentage of the cross-sectional area of the spinal cord covered by axons, and the major and minor axes of elliptical approximations of axons with non-circular cross-sections. Figure 2.14D shows the outlines and numbering of each axon, that were produced using ImageJ.

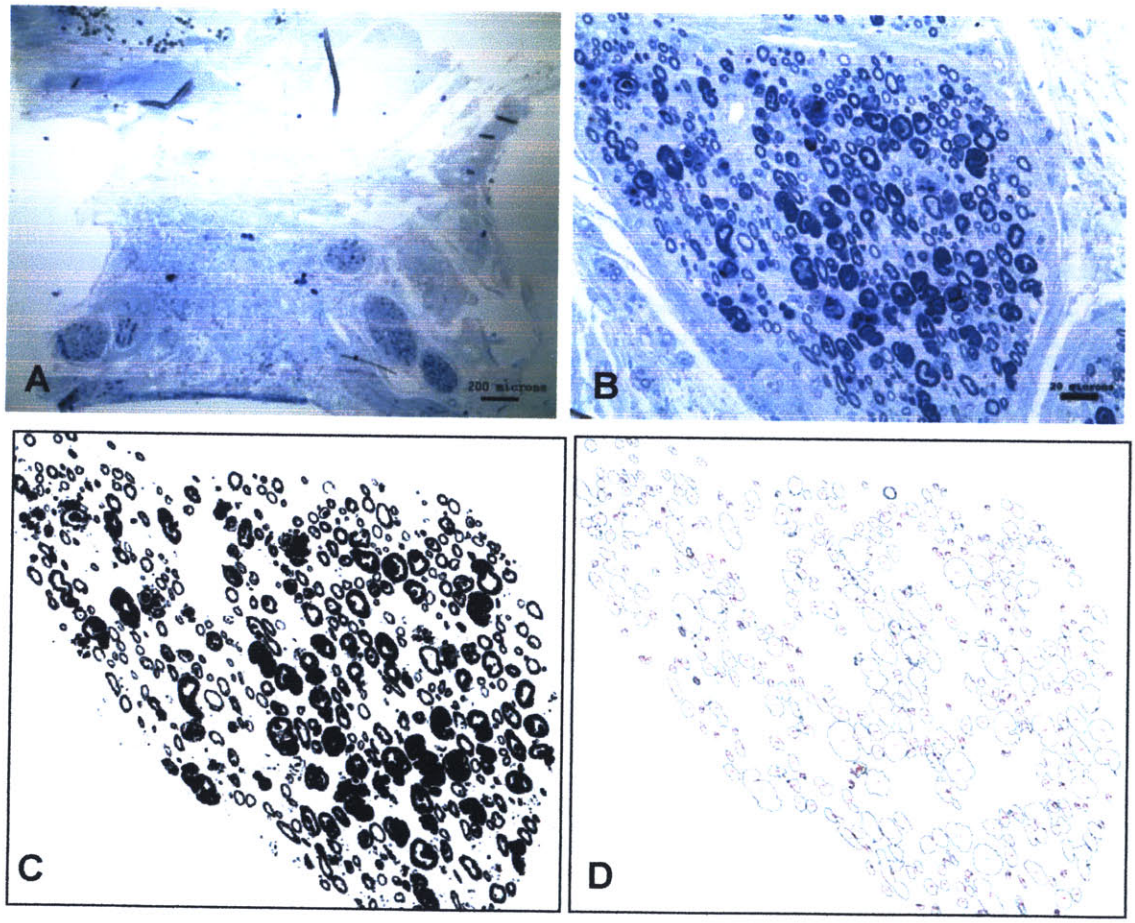


**Figure 2.14** – (A) Cross-section of the center of the lesion of a control animal (no implantation) (40x). (B) 200x magnification of the lesion center. (C) High contrast black and white image of spinal cord section. (D) Numerical labeling and outlining of individual axons.

## Chapter 3: Results

### 3.1 Survival Post-Surgery

A total of 36 rats (28 Sprague Dawley (SD) and 8 Lewis) underwent surgery. Only 1 SD and 1 Lewis rat died during the operation; however a total of 11 SD rats died post-operatively. In general, the rats that did not survive, died within a few days after surgery. A couple animals died after a few weeks due to bladder infection. Eleven SD rats exhibited self-mutilation; 3 of which were euthanized due to the mutilation. None of the Lewis rats died post-operatively and none exhibited self-mutilation. The number of rats from each experimental group which survived for six weeks after surgery is show in Table 3.1.

**Table 3.1** – Experimental Groups

| **Group: Implant Type** | **Number of Rats** |
|---|---|
| Group I: Control (no implant) | 8 (SD) |
| Group II: Collagen membrane used as dorsal barrier | 7 (SD) |
| Group III: Collagen membrane used as a wrap | 4 (SD) |
| Group IV: Collagen tube spilt longitudinally (opening of tube on dorsal side of spinal cord) | 7 (Lewis) |

. All the rats exhibited complete hindlimb paralysis following surgery and moved about their cages by exclusive use of their forelimbs.

### 3.2 Functional Ability

Digital video recording of rat ambulation was taken for all animals at 6 weeks post operatively. Although no formal grading system was used to assess motor function; no discernable differences in functional recovery were noticeable among the four experimental groups based on our general observations. Animals from all groups showed slight uncoordinated hind limb motion without significant weight bearing ability. Figure 3.1 (top) shows three consecutive snapshots taken 0.5 seconds apart of a video recording of a tube implanted rat. Figure 3.1 (bottom) shows three consecutive snapshots taken 0.5 seconds apart of a video recording of a normal Lewis rat (no spinal cord injury).

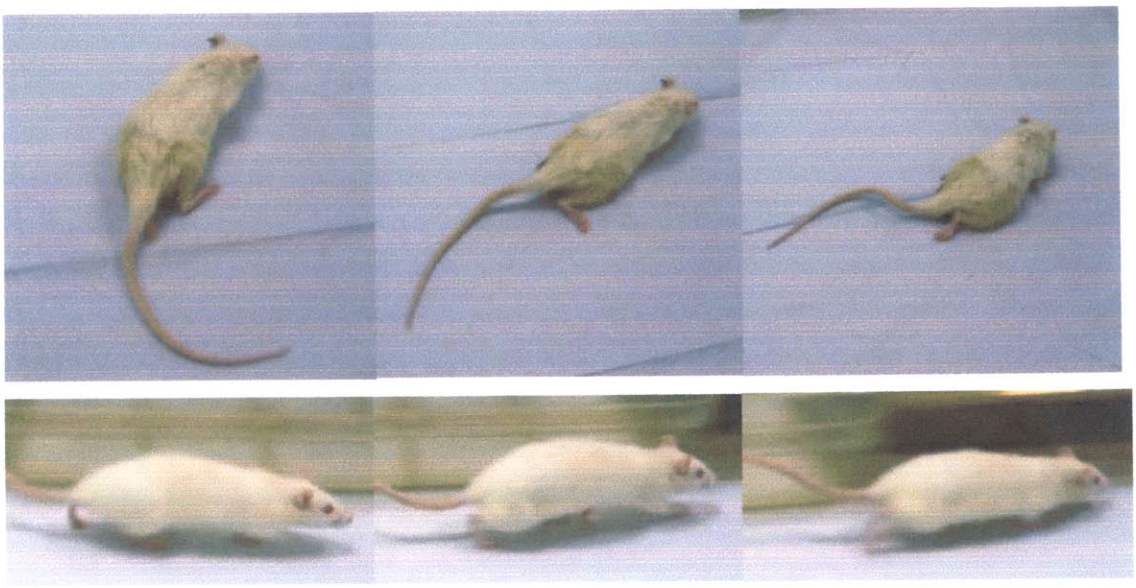

**Figure 3.1** – Three consecutive snapshots (left to right) taken 0.5 seconds apart of a tube implanted rat (top) and a normal (no spinal cord injury) rat (bottom).

### 3.3 Morphological Observations

Six weeks after surgery, extraction of the rat spinal cords revealed reparative tissue completely filling the 5 mm gap created by spinal cord transection in all of the experimental groups. The tissue at the center of the defect in all animals lacked the normal spinal cord anatomy, which is comprised of distinct areas of gray and white matter. Images taken of the cross-sections of plastic embedded spinal cord defect areas were analyzed using ImageJ to determine defect-center cross-sectional areas and aspect ratios. The cross-sectional areas of the center of the defect of the four experimental groups are shown in Figure 3.2. The cross-sectional area of a normal SD adult rat spinal cord was found to be approximately 4.5 $mm^2$; indicated by the dashed line in Figure 3.2. Groups I, III, and IV had cross-sections slightly less than normal. The average cross-sectional area in Group II was approximately the same as normal.

The aspect ratio is a measure of the circularity of the cross-section; where a perfect circle has an aspect ratio of 1. In non-circular cross-sections, the aspect ratio is the ratio of the major axis divided by the minor axis (i.e. long diameter/short diameter). The aspect ratio of a normal adult SD rat spinal cord cross-section in the thoracic region of the spine is approximately 1.1. A comparison of the average aspect ratios of the four

experimental groups is shown in Figure 3.3. The group with the smallest aspect ratio (i.e. most circular cross-section) was the tubular implant group (Group IV). The group with the largest aspect ratio (and also the largest cross-sectional area) was Group II.

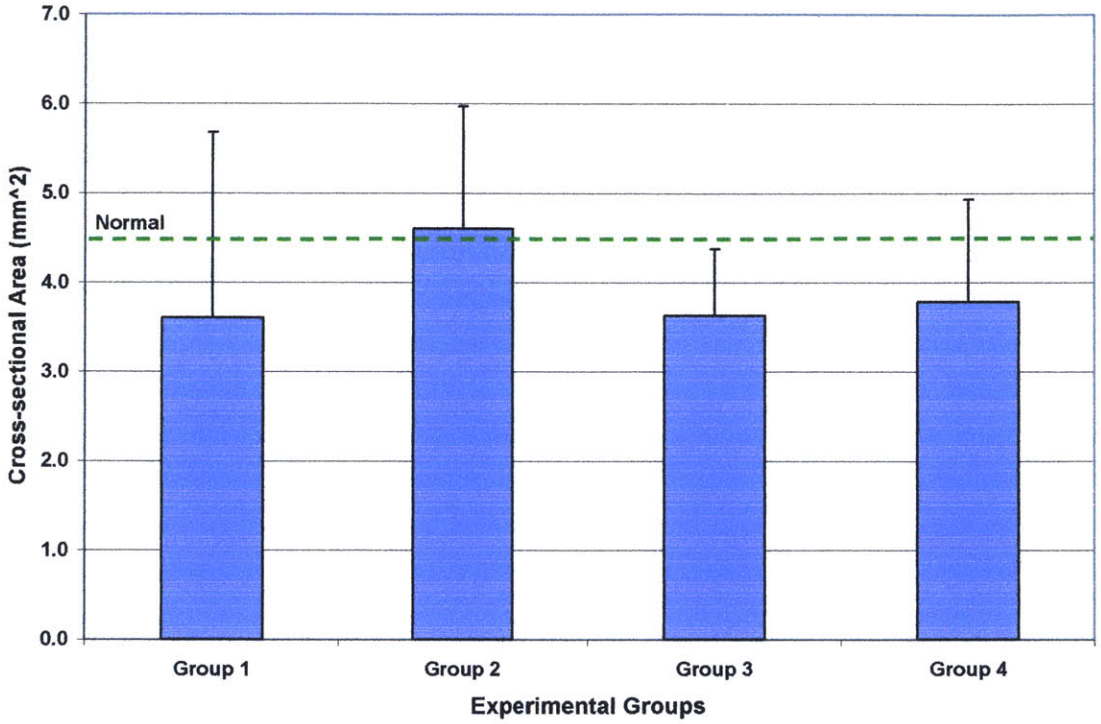


**Figure 3.2** – Graph comparing average cross-sectional areas of the lesion centers for the four experimental groups. Dashed line indicates cross-sectional area of a normal rat.

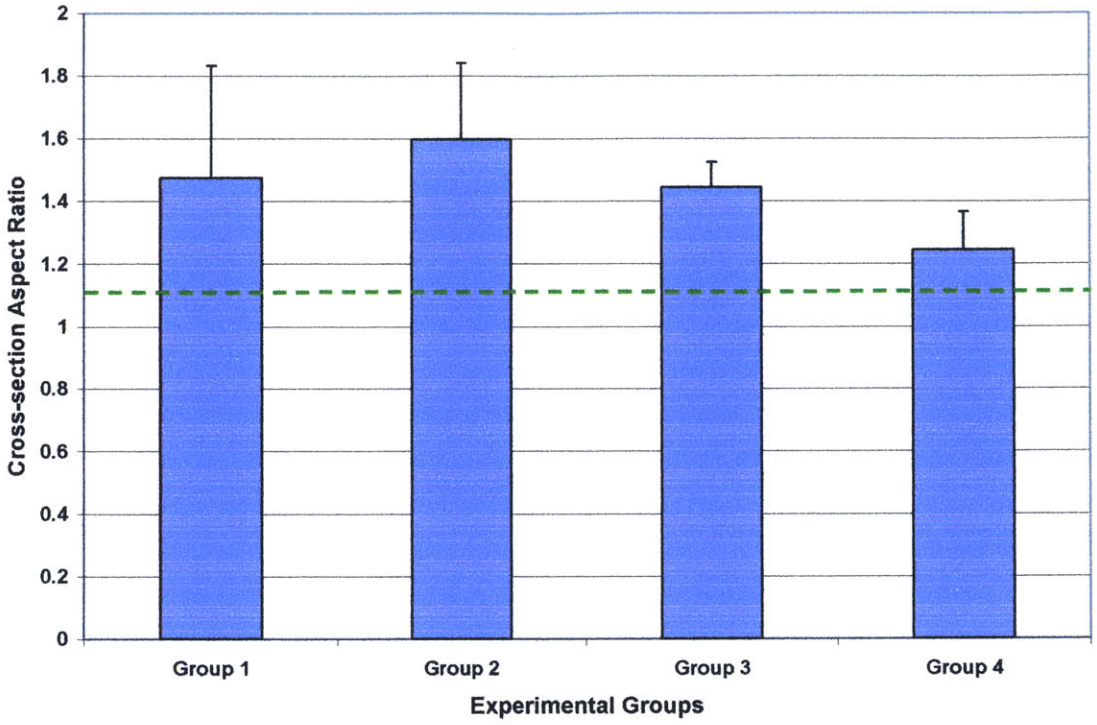


**Figure 3.3** – Graph comparing the aspect ratios of the lesion center cross-sections.

### 3.4 Histological Findings

Longitudinal sections were taken of the paraffin embedded spinal cord segment rostral to the defect-center. These sections were stained with H & E for general cell identification and Masson's Trichrome to identify the presence of collagenous tissue (Figure 3.4). Transverse sections of the defect-center were stained with osmium tetroxide and toluidine blue for axon quantification (Figure 3.4). The transverse sections were also used for general morphological observations. Longitudinal and transverse sections of a normal (uninjured) thoracic level rat spinal cord are shown in Figure 3.5.

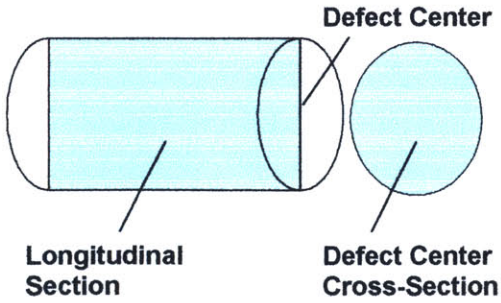


**Figure 3.4** – Sectioning strategy. Longitudinal sections were stained with H&E or Masson's Trichrome. Defect center cross-sections were stained with osmium tetroxide and toluidine blue.

H & E staining showed the presence of large cysts filling the defect areas of Groups I

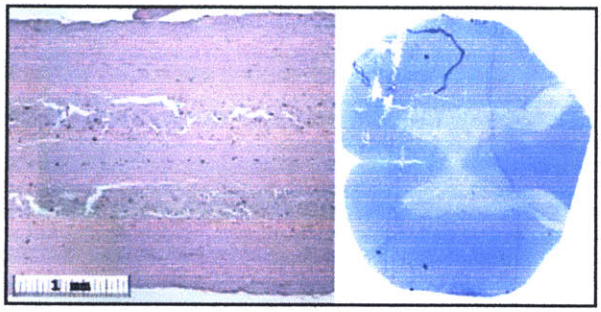

**Figure 3.5** – Normal rat spinal cord. Longitudinal section (left) stained with H&E. Transverse section (right) stained with toluidine blue.

and II, while groups III and IV demonstrated less extensive cyst formation (Figures 3.6-3.9). At the interface between the rostral spinal cord stump and the reparative tissue in the gap there was a marked accumulation of cells, possibly astrocytes and macrophages, in all four groups. Acute inflammatory cells (polymorphonuclear neutrophils, basophils, and eosinophils) were not observed in any of the groups, which indicates an absence of an immune response to the collagen implants. Masson's trichrome showed a high degree of dense collagenous tissue within the defect of groups I through IV, while H & E revealed fibroblasts with their characteristic elongated morphology dispersed within the collagenous extracellular matrix. In Groups I and II the orientation of the collagen fibers tended to be in a transverse direction (Figure 3.10A). The collagen fibers in Group III tended to be more longitudinally oriented, and even more so in Group IV (Figure 3.10B).

After six weeks, the collagen implants in Groups II - IV underwent considerable degradation; however, disintegrating portions of the collagen implants were visible in Groups III and IV (wrap and tube). Remnants of the wrap were highly visible (Figure 3.8), even though considerable fragmentation of the wall of the wrap occurred, whereas only small remains of the tube could be seen.

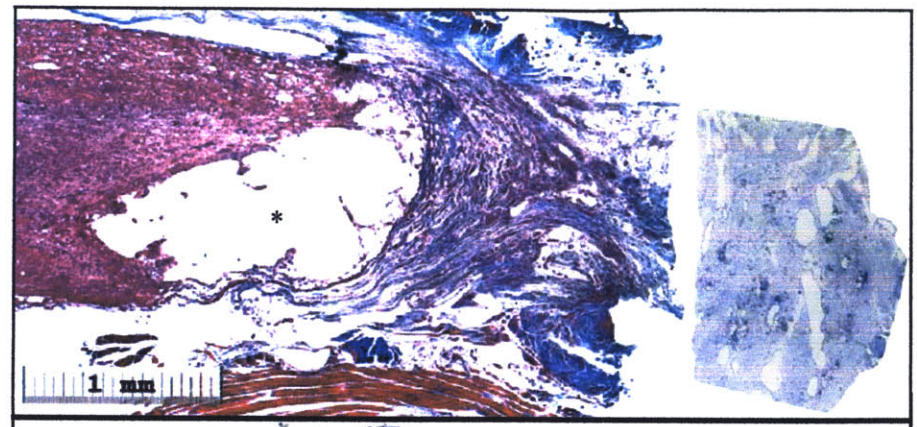


**Figure 3.6** – Explanted spinal cord of control animal showing a large cyst (*) at the interface between the defect and undamaged cord. Longitudinal section (left) stained with Masson's Trichrome. Transverse section of defect center (right) stained with toluidine blue.

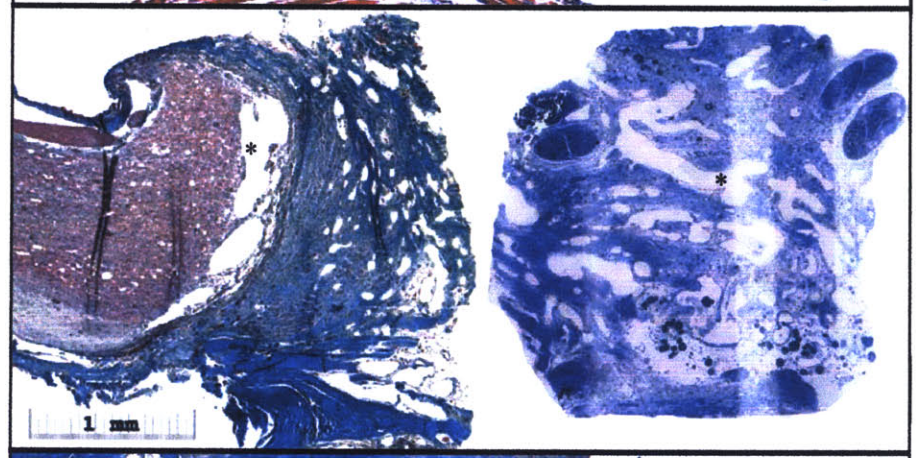


**Figure 3.7** – Explanted spinal cord of Group II rat showing numerous cysts (*) filling the defect. Longitudinal section (left) stained with Masson's Trichrome. Transverse section of defect center (right) stained with toluidine blue.

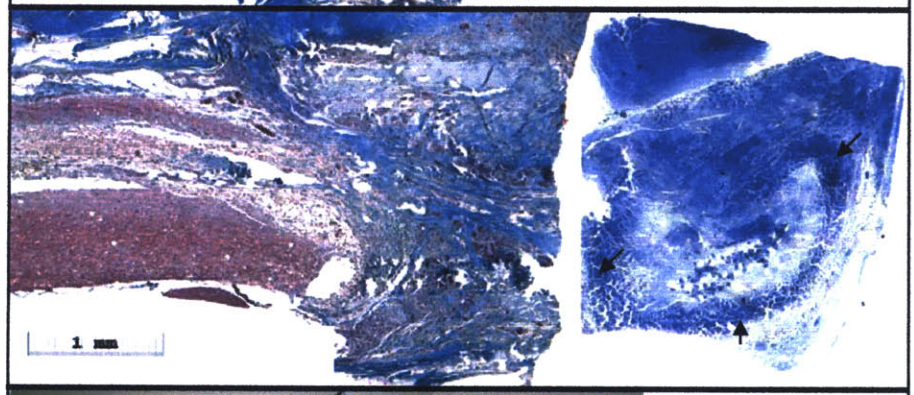


**Figure 3.8** – Explanted spinal cord of Group III (wrap) rat showing improved integration of tissue within the defect and adjacent undamaged spinal cord. Remains of the collagen wrap are clearly visible in transverse section (arrows). Long. section (left) stained with Masson's Trich. Trans. section (right) stained with toluidine blue.

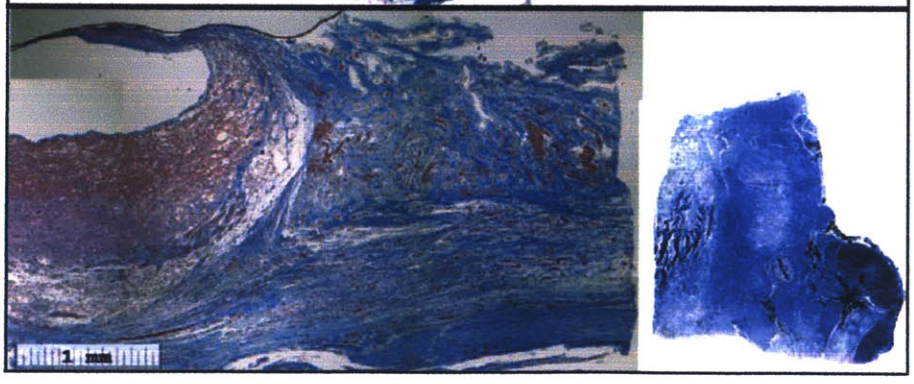

**Figure 3.9** – Explanted spinal cord of Group IV (tube) rat demonstrating fewer cysts within the defect. Longitudinal section (left) stained with Masson's Trichrome. Transverse section of defect center (right) stained with toluidine blue.

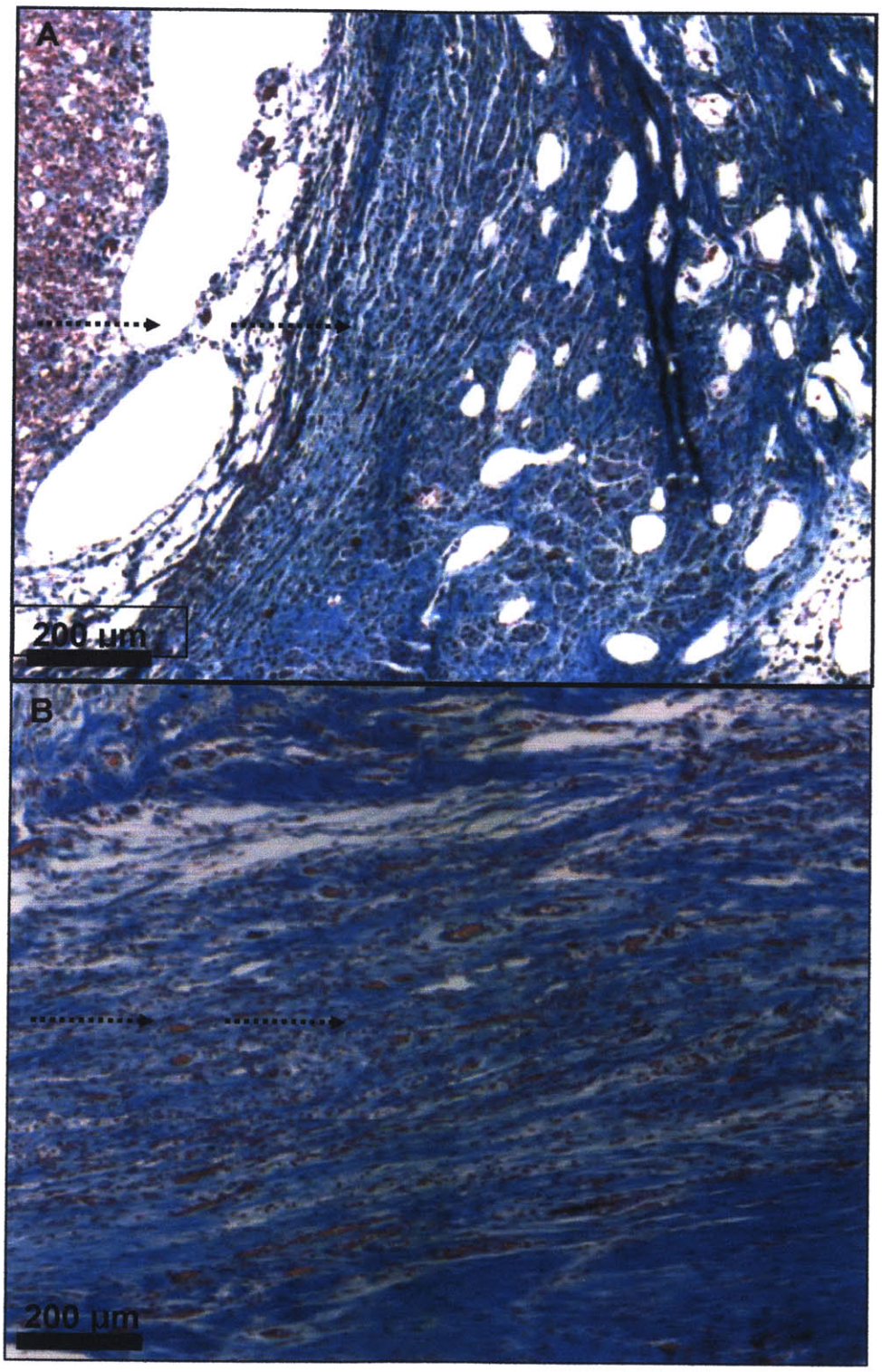


**Figure 3.10** – High magnification of the defect center showing a highly collagenous tissue composition. (A) The group with only the dorsal barrier implanted showed the collagenous tissue within the gap orientated transverse to the spinal cord axis (arrows). (B) The group with the tubular implant showed the tissue within the defect to be closely aligned with the spinal cord axis. Paraffin embedded sections were stained with Masson's trichrome which stains collagen blue, cellular material red, and cell nuclei purple.

### 3.5 Axonal quantification

Myelinated axons at the center of the defect were identified by post-fixing the caudal segments of the spinal cord explants in 1% osmium tetroxide to stain for myelin. Toluidine blue staining of the sections was also done, to provide better contrast of the tissue. High resolution images (200x) taken under light microscopy were used to observe myelinated axons, which were found in all four experimental groups. In groups I and II regenerated axons were often found in high density bundles, or fascicles on the periphery of the defect cross-section (see Figures 3.11 and 3.12). In contrast, the axons in groups III and IV were not found in fascicles, but were generally spread across the cross-sectional area (see Figure 3.13 and 3.14).

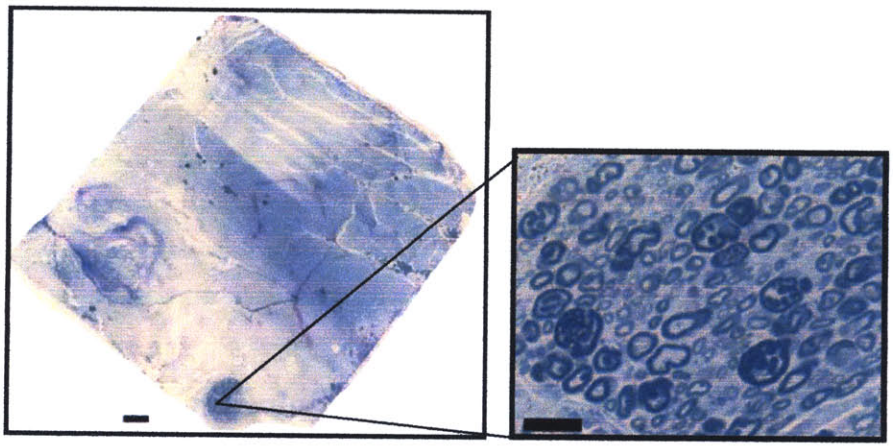

**Figure 3.11** – Left: The cross-section of the defect-center of a control animal (scale bar = 200 μm). Right: a high magnification image of myelinated axons found within a large fascicle on the periphery of the cross-section (scale bar = 20 μm).

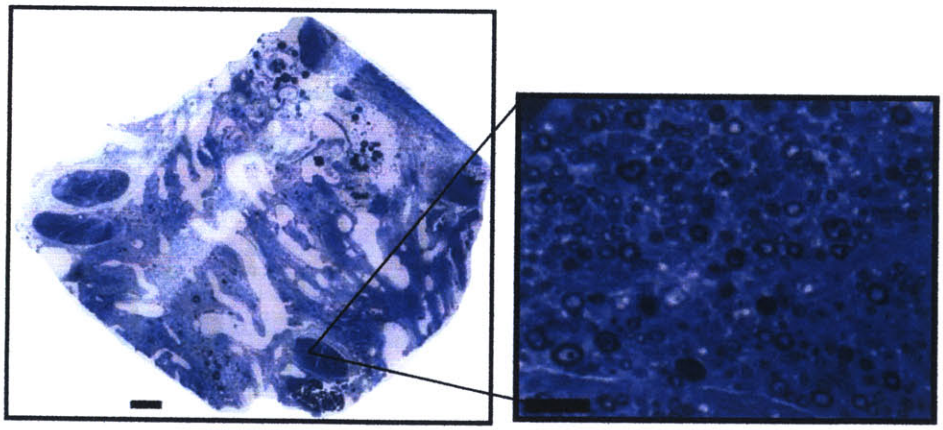

**Figure 3.12** - Left: The cross-section of the defect-center of a dorsal barrier implanted animal (scale bar = 200 μm). Right: a high magnification image of myelinated axons found within a large fascicle on the periphery of the cross-section (scale bar = 20 μm).

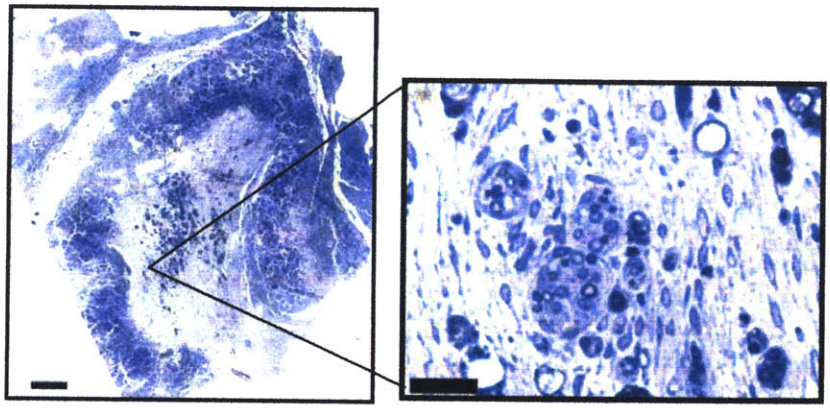

**Figure 3.13** - Left: The cross-section of the defect-center of a wrap implanted animal (Group III) (scale bar = 200 μm). Axons in this group were not found in large fascicles but were generally spread across various areas of the defect. Right: a high magnification image of myelinated axons found in the central region of the defect (scale bar = 20 μm).

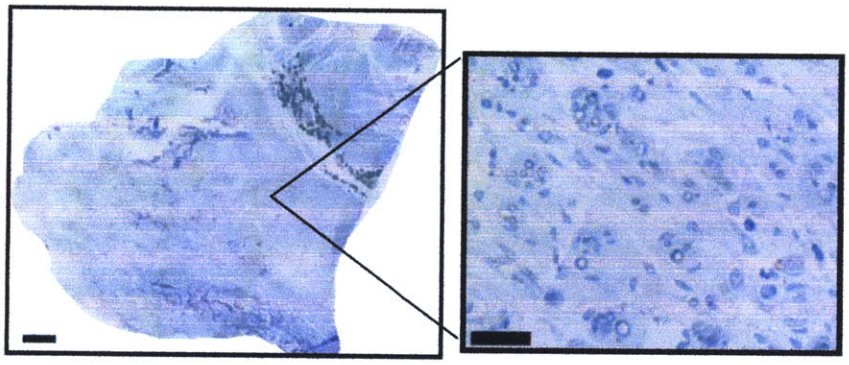

**Figure 3.14** - Left: The cross-section of the defect-center of a tube implanted animal (Group IV) (scale bar = 200 μm). Axons in this group were not found in large fascicles but were generally spread across various areas of the defect. Right: a high magnification image of myelinated axons found in the central region of the defect (scale bar = 20 μm).

The total number of axons found at the defect-center in each group is shown in Figure 3.15; the error bars indicate standard deviation. Interestingly, the number of axons found was similar among the three implant groups and the control group; ranging between 1000 and 1700 axons. A one-way Analysis of Variance (ANOVA) test showed no statistical significance between the mean values of each group ($P > 0.05$). In comparison, the number of axons in the thoracic region of a normal rat (without spinal cord injury) was found to be approximately 130,000.

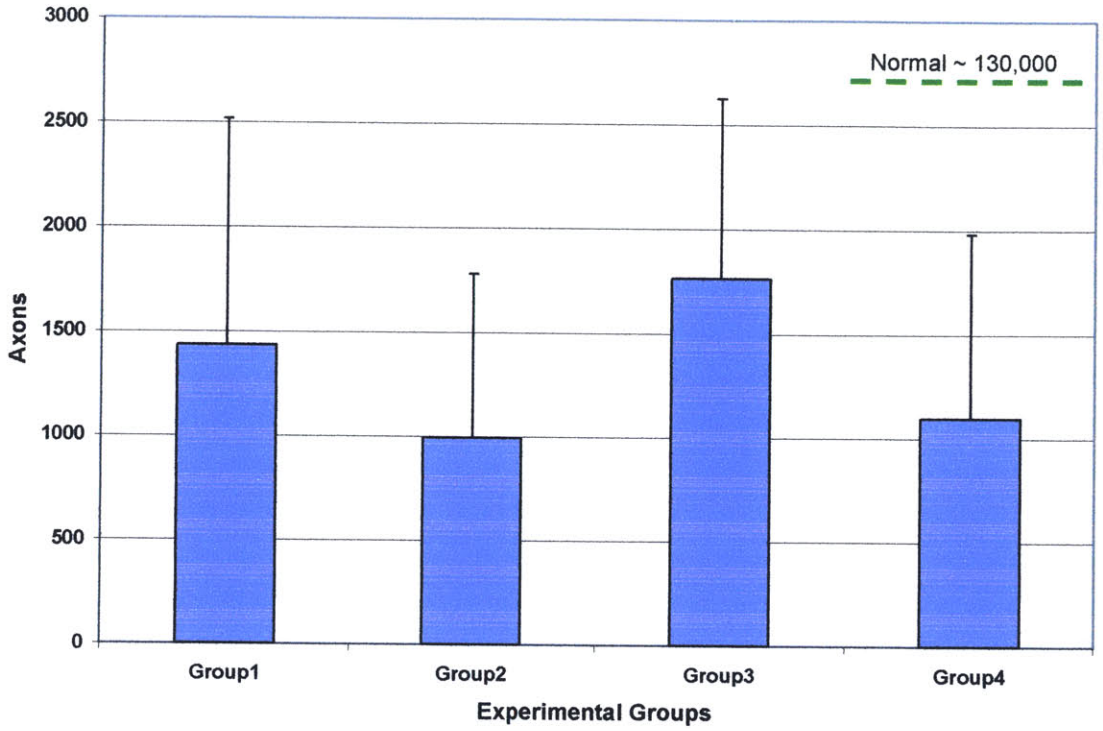


**Figure 3.15-** Graph showing the mean number of axons found at the lesion center.

Analysis of the aspect ratios of the axons found within the gap showed that all the groups had mean aspect ratios near 2 ($P > 0.05$). The aspect ratios were $2.04 \pm 0.25$ (mean $\pm$ SD, n=8), $1.83 \pm 0.17$ (n=7), $2.13 \pm 0.336$ (n=4) and $1.98 \pm 0.25$ (n=7) for groups I through IV respectively.

## Chapter 4: Discussion

The objective of this study was to investigate the effects that collagen implants have on the regeneration of the adult rat spinal cord. Three implants were evaluated including a thin collagen membrane used as a dorsal barrier to overlaying soft tissue covering a 5 mm gap in the spinal cord, the same collagen membrane used as a wrap to enclose the ends of the cord stumps, and lastly a collagen tube that was opened longitudinally and used as a bridge between the two cord stumps.

Each of the evaluated implants provided containment of the defect by preventing the invasion of surrounding tissue into the spinal cord gap. Invading tissue acts as a barrier to axons trying to cross the lesion. Tubular shaped implants provided a unique enclosure which could be beneficial for controlling the environment of the lesion.

Histological analysis showed a large amount of collagenous tissue filling the defect gap of all animals 6 weeks after surgery. The control group and dorsal barrier implanted group showed significant numbers of large fluid-filled cysts within the defect; whereas cysts were largely absent from the wrap and tube implanted groups. There were also notable differences in the orientation of the scar tissue within the gaps of tubular and non-tubular groups. The scar tissue in the tubular groups tended to be considerably inline with the axis of the spinal cord; whereas the control and dorsal barrier groups had scar tissue oriented transverse to the spinal cord axis. These findings are consistent with the results published by Spilker et al. who found a similar difference in scar orientation between tubular and non-tubular implanted animals [35].

The complete transection model (and removal of nearby peripheral nerve roots) ensures that all ascending and descending axons are disrupted. Therefore, any axons found at the defect-center can be assumed to be regenerated axons. Images taken at high magnification of myelin stained cross-sections of the defect, revealed distinctive patterns of regenerated axons at the defect-center of the different groups. In the control and dorsal barrier groups, a large number of the regenerating axons were found in large fascicles on the periphery of the cross-section. This was in stark contrast to the pattern seen in the wrap and tube groups, where the regenerated axons were found spread across different areas of the defect cross-section. It was not possible to determine the origin of the regenerated axons and it is likely that some, if not many, of the axons were ascending

tract axons originating in the peripheral nervous system. This is consistent with the identification of well defined fascicules in groups I and II on the periphery of the defect cross-section. The tubular implant groups are less likely to support the in-growth of peripheral nerve originating axons due to the tubular construct acting as a wall to the adjacent severed peripheral nerve roots.

The quantification of myelinated axons found at the defect-center revealed a notable number of regenerated axons penetrating the defect in all of the experimental groups. The differences among the total number of regenerated axons in each group was not significant. Similarly, there was little difference in the mean aspect ratios of the regenerated axons from each group; with the mean aspect ratio being approximately 2 in all groups. These results concur to some extent with those published by Spilker et al. [35] who found no significant difference in the number of regenerated axons in tubular and non-tubular implanted groups; however, Spilker et al. reported differences in the aspect ratios of the axons in tubular and non-tubular groups.

## Chapter 5: Conclusion

Damage to the spinal cord results in an extremely hostile environment for axonal regeneration. Notwithstanding, tubular shaped collagen based implants help counter adverse conditions within the defect by reducing the formation of large fluid-filled cysts and providing more favorable organization of the scar tissue by aligning the tissue closely with the axis of the spinal cord. The tubular implants were supportive of axonal regeneration within the defect, and the number of regenerated axons found within all of the groups is encouraging.

Even so, it is clear that a multifaceted approach is necessary to effectively facilitate satisfactory regeneration of the spinal cord. This may include the use of stem cells, growth factors, and a porous cylindrical scaffold. The collagen implants investigated in the current study (i.e. dorsal barrier and/or tubular implants) could provide a working platform for the incorporation of these additional therapies.

**Appendix A: Dehydrothermal Crosslinking Protocol (adapted from Harley, 2002)**

1. Place collagen material in aluminum foil packet. Leave packet open at top.
2. Place packet in vacuum oven (Isotemp Model 201, Fisher Scientific, Boston, MA).
3. Turn on vacuum. The vacuum oven should reach a final pressure of approximately 29.7 mmHg. Leave the matrix in the oven for 24 hours at 105°C.
4. At the end of the exposure period, turn off the vacuum and vent the chamber. Open the vacuum door and immediately seal the aluminum foil bags. The matrix is now crosslinked and considered sterile, so the matrix should only be handled under sterile conditions from now on.
5. Store the matrix in a dessicator. Crosslinked matrices can remain indefinitely in a dessicator prior to testing or use.

**Appendix B: Plastic Embedding Protocol**

SOLUTIONS:

Cacodylate Buffer (pH 7.4)

Stock Solutions:

*Stock A: 0.2 M Sodium Cacodylate in liquid form (pH 7.4)*
*(Catalog No. 18661, Polysciences, Inc., Warrington, PA)*

*Final Molar Composition of Buffer (Working Solution):*
*50 ml of Stock A + 50 ml of Distilled Water*
*Gives 0.1 M Sodium Cacodylate (pH 7.4)*

OR

| | |
|---|---|
| Stock A (0.2 M Sodium Cacodylate - mw 214): | 4.28 grams Sodium Cacodylate (powder)<br>100 ml of Distilled Water |
| Stock B (0.2 M HCl - mw 36.46): | 1.7 ml HCl<br>100 ml of Distilled Water |

* = Volume of Stock B changes for different pH levels

Composition of Buffer:
50 ml of Stock A + 1.4 ml of Stock B (for pH 7.4)* + 48.6 ml Distilled Water
* = Volume of Stock B changes for different pH levels

Final Molar Composition of Buffer:
0.1M Sodium Cacodylate
0.0028M HCl

Cacodylate Buffered Glutaraldehyde

| | |
|---|---|
| 2% Solution: | 8 ml 25% Glutaraldehyde<br>92 ml working cacodylate Buffer |

Osmium Tetroxide Solution (Catalog No. 251755, Sigma-Aldrich, St. Louis,MO)

| | |
|---|---|
| 1% Solution: | 2 ml 4% Osmium Tetroxide<br>6 ml working cacodylate buffer |

Note: Can use 1-2% Osmium Tetroxide in 0.1M buffer

Poly/Bed 812 Embedding Kit (Catalog No. 08792, Polysciences, Inc., Warrington, PA)
Half Portion:

| | Catalog # | Standard Formula | Slightly Harder |
|---|---|---|---|

| | | | |
|---|---|---|---|
| Poly/Bed 812 | 08791 | 24 ml | 23.5 ml |
| DDSA | 00563 | 15.5 ml | 14.3 ml |
| NMA | 00886 | 10.5 ml | 12.0 ml |
| DMP-30* | 00553 | 1.0 ml | 1.0 ml |

EMBEDDING PROCEDURE

1. Soak nerves in 2% cacodylate buffered glutaraldehyde 2-4 hours at 4°C (or on ice).

2. Rinse nerves 3 times in 0.1 M working cacodylate buffered solution, 5 min each.

3. Fix in 1-2% osmium tetroxide solution for 1-2 hours at room temperature (in the hood) in dark.

4. Rinse nerves 3 times in 0.1 M working cacodylate buffered solution, 5 min each.

*Can hold here (at 4°C) for a few days if necessary*

5. Dehydrate nerves in Reagent Alcohol:

| | |
|---|---|
| 70% | 5 minutes |
| 80% | 10 minutes |
| 90% | 10 minutes |
| 90% | 10 minutes |
| 100% | 10 minutes |
| 100% | 10 minutes |
| 100% | 10 minutes |

6. Clear nerves in acetone 2 times, 5 minutes for first exposure, 10 minutes for second.

> BEWARE: Use fresh acetone for procedure. Acetone tends to pick up water overtime, resulting in the formation of micro-pockets of water along surface of nerve, impeding Epon infiltration.

7. Infiltrate in 1:1 acetone/Epon mixture at room temperature for 5-24 hrs (rotate).

8. Infiltrate in 100% Epon 8 hours at room temperature (rotate).

9. Embed in TEM molds (with fresh 100% Epon).

10. Let cure 24 hours at 60°C in oven (standard pressure).

**Appendix C: Hematoxylin and Eosin (H & E) Staining Protocol**

Formalin fixed, paraffin embedded specimens

**Solutions**

| | | |
|---|---|---|
| Hematoxylin | Harris Hematoxylin Solution, Sigma Cat# HHS-128. of stock solution into staining dish. | Filter 200ml |
| Eosin | Eosin Y Solution Aqueous, Sigma Cat# HT110-2-128 | |
| Acid Alcohol | 0.5 % in 80% alcohol (99.5ml of 80% alcohol + 0.5 ml HCl) | |

**Other Materials**

| | |
|---|---|
| Cytoseal | Cytoseal 60, Cat# 18006, Electron Microscopy Sciences. |

**Methods**

1. Deparaffinize and Rehydrate

| | |
|---|---|
| Xylene (or substitute) | 2 x 5 min. |
| 100% alcohol | 2 x 3 min. |
| 95% alcohol | 2 x 2min. |
| 80% alcohol | 1 min. |
| Wash in tap water | 5 min. |

2. Hematoxylin, 3 min. Note: be sure to filter hematoxylin prior to use!
3. Wash in tap water for 5 min.
4. One quick dip in acid alcohol.
5. Wash in tap water for 5 min.
6. Eosin, 3 quick dips.
7. Dehydrate

| | |
|---|---|
| 100% alcohol | 2 x 3 min. |
| Xylene (or substitute) | 2 x 3 min. |

8. Coverslip with Cytoseal

**References**


1. *Spinal cord injury. Facts and figures at a glance.* J Spinal Cord Med, 2005. **28**(4): p. 379-80.
2. Kirshblum, S., et al., *Physical Medicine and Rehabilitation Board Review*, ed. S.J. Cuccurullo. 2004: Demos Medical Publishing, Inc.
3. Martin, J.H., *Neuroanatomy : text and atlas*. 2nd ed. 1996, Stamford, Conn.: Appleton & Lange. xxiii, 578 p.
4. Afifi, A.K. and R.A. Bergman, *Functional neuroanatomy : text and atlas*. 1998, New York: McGraw-Hill, Health Professions Division. xii, 730 p.
5. Kiernan, J.A. and M.L. Barr, *Barr's The human nervous system : an anatomical viewpoint*. 8th ed. 2005, Philadelphia: Lippincott Williams & Wilkins. viii, 469 p.
6. Hagg, T. and M. Oudega, *Degenerative and spontaneous regenerative processes after spinal cord injury.* J Neurotrauma, 2006. **23**(3-4): p. 263-80.
7. Buss, A., et al., *Sequential loss of myelin proteins during Wallerian degeneration in the human spinal cord.* Brain, 2005. **128**(Pt 2): p. 356-64.
8. Bracken, M.B., *Treatment of acute spinal cord injury with methylprednisolone: results of a multicenter, randomized clinical trial.* J Neurotrauma, 1991. **8 Suppl 1**: p. S47-50; discussion S51-2.
9. Trivedi, J.M., *Spinal trauma: therapy--options and outcomes.* Eur J Radiol, 2002. **42**(2): p. 127-34.
10. Woerly, S., et al., *Prevention of gliotic scar formation by NeuroGel allows partial endogenous repair of transected cat spinal cord.* J Neurosci Res, 2004. **75**(2): p. 262-72.
11. Suzuki, Y., et al., *Electrophysiological and horseradish peroxidase-tracing studies of nerve regeneration through alginate-filled gap in adult rat spinal cord.* Neurosci Lett, 2002. **318**(3): p. 121-4.
12. Yoshii, S., et al., *Restoration of function after spinal cord transection using a collagen bridge.* J Biomed Mater Res A, 2004. **70**(4): p. 569-75.
13. Harley, B.A., et al., *Optimal degradation rate for collagen chambers used for regeneration of peripheral nerves over long gaps.* Cells Tissues Organs, 2004. **176**(1-3): p. 153-65.
14. Kuh, S.U., et al., *Functional recovery after human umbilical cord blood cells transplantation with brain-derived neutrophic factor into the spinal cord injured rat.* Acta Neurochir (Wien), 2005. **147**(9): p. 985-92.
15. Cummings, B.J., et al., *Human neural stem cells differentiate and promote locomotor recovery in spinal cord-injured mice.* Proc Natl Acad Sci U S A, 2005. **102**(39): p. 14069-74.
16. Cao, Q., et al., *Functional recovery in traumatic spinal cord injury after transplantation of multineurotrophin-expressing glial-restricted precursor cells.* J Neurosci, 2005. **25**(30): p. 6947-57.
17. Tohill, M., et al., *Rat bone marrow mesenchymal stem cells express glial markers and stimulate nerve regeneration.* Neurosci Lett, 2004. **362**(3): p. 200-3.
18. Ankeny, D.P., D.M. McTigue, and L.B. Jakeman, *Bone marrow transplants provide tissue protection and directional guidance for axons after contusive spinal cord injury in rats.* Exp Neurol, 2004. **190**(1): p. 17-31.

19. Wu, S., et al., *Bone marrow stromal cells enhance differentiation of cocultured neurosphere cells and promote regeneration of injured spinal cord.* J Neurosci Res, 2003. **72**(3): p. 343-51.
20. Hofstetter, C.P., et al., *Marrow stromal cells form guiding strands in the injured spinal cord and promote recovery.* Proc Natl Acad Sci U S A, 2002. **99**(4): p. 2199-204.
21. Lu, P., L.L. Jones, and M.H. Tuszynski, *BDNF-expressing marrow stromal cells support extensive axonal growth at sites of spinal cord injury.* Exp Neurol, 2005. **191**(2): p. 344-60.
22. Lopez-Vales, R., et al., *Acute and delayed transplantation of olfactory ensheathing cells promote partial recovery after complete transection of the spinal cord.* Neurobiol Dis, 2006. **21**(1): p. 57-68.
23. Ramon-Cueto, A., et al., *Long-distance axonal regeneration in the transected adult rat spinal cord is promoted by olfactory ensheathing glia transplants.* J Neurosci, 1998. **18**(10): p. 3803-15.
24. Ramer, L.M., et al., *Peripheral olfactory ensheathing cells reduce scar and cavity formation and promote regeneration after spinal cord injury.* J Comp Neurol, 2004. **473**(1): p. 1-15.
25. Ruitenberg, M.J., et al., *NT-3 expression from engineered olfactory ensheathing glia promotes spinal sparing and regeneration.* Brain, 2005. **128**(Pt 4): p. 839-53.
26. Teng, Y.D., et al., *Functional recovery following traumatic spinal cord injury mediated by a unique polymer scaffold seeded with neural stem cells.* Proc Natl Acad Sci U S A, 2002. **99**(5): p. 3024-9.
27. Vacanti, M.P., et al., *Tissue-engineered spinal cord.* Transplant Proc, 2001. **33**(1-2): p. 592-8.
28. Iwata, A., et al., *Long-term survival and outgrowth of mechanically engineered nervous tissue constructs implanted into spinal cord lesions.* Tissue Eng, 2006. **12**(1): p. 101-10.
29. Liebscher, T., et al., *Nogo-A antibody improves regeneration and locomotion of spinal cord-injured rats.* Ann Neurol, 2005. **58**(5): p. 706-19.
30. Koprivica, V., et al., *EGFR activation mediates inhibition of axon regeneration by myelin and chondroitin sulfate proteoglycans.* Science, 2005. **310**(5745): p. 106-10.
31. Kim, J.E., et al., *Axon regeneration in young adult mice lacking Nogo-A/B.* Neuron, 2003. **38**(2): p. 187-99.
32. Shapiro, S., et al., *Oscillating field stimulation for complete spinal cord injury in humans: a phase 1 trial.* J Neurosurg Spine, 2005. **2**(1): p. 3-10.
33. Chamberlain, L.J., et al., *Collagen-GAG substrate enhances the quality of nerve regeneration through collagen tubes up to level of autograft.* Exp Neurol, 1998. **154**(2): p. 315-29.
34. Chamberlain, L.J., et al., *Near-terminus axonal structure and function following rat sciatic nerve regeneration through a collagen-GAG matrix in a ten-millimeter gap.* J Neurosci Res, 2000. **60**(5): p. 666-77.
35. Spilker, M.H., et al., *The effects of tubulation on healing and scar formation after transection of the adult rat spinal cord.* Restor Neurol Neurosci, 2001. **18**(1): p. 23-38.

36. Spilker, M.H., et al., *The effects of collagen-based implants on early healing of the adult rat spinal cord.* Tiss. Engr., 1997. **3**: p. 309-317.
37. Talac, R., et al., *Animal models of spinal cord injury for evaluation of tissue engineering treatment strategies.* Biomaterials, 2004. **25**(9): p. 1505-10.
38. Carmel, J.B., et al., *Gene expression profiling of acute spinal cord injury reveals spreading inflammatory signals and neuron loss.* Physiol Genomics, 2001. **7**(2): p. 201-13.
39. Chamberlain, L.J., et al., *Early peripheral nerve healing in collagen and silicone tube implants: myofibroblasts and the cellular response.* Biomaterials, 1998. **19**(15): p. 1393-403.
40. Chamberlain, L.J., et al., *Connective tissue response to tubular implants for peripheral nerve regeneration: the role of myofibroblasts.* J Comp Neurol, 2000. **417**(4): p. 415-30.
41. Carr, M.M., et al., *Strain differences in autotomy in rats undergoing sciatic nerve transection or repair.* Ann Plast Surg, 1992. **28**(6): p. 538-44.
42. Shir, Y., et al., *Correlation of intact sensibility and neuropathic pain-related behaviors in eight inbred and outbred rat strains and selection lines.* Pain, 2001. **90**(1-2): p. 75-82.